Universiteit Leiden
The Netherlands

Colonization of the live biotherapeutic product VE303 and modulation of the microbiota and metabolites in healthy volunteers

Dsouza, M.; Menon, R.; Crossette, E.; Bhattarai, S.K.; Schneider, J.; Kim, Y.G.; … ; Norman, J.M.

Colonization of the live biotherapeutic product VE303 and modulation of the microbiota and metabolites in healthy volunteers

Graphical abstract
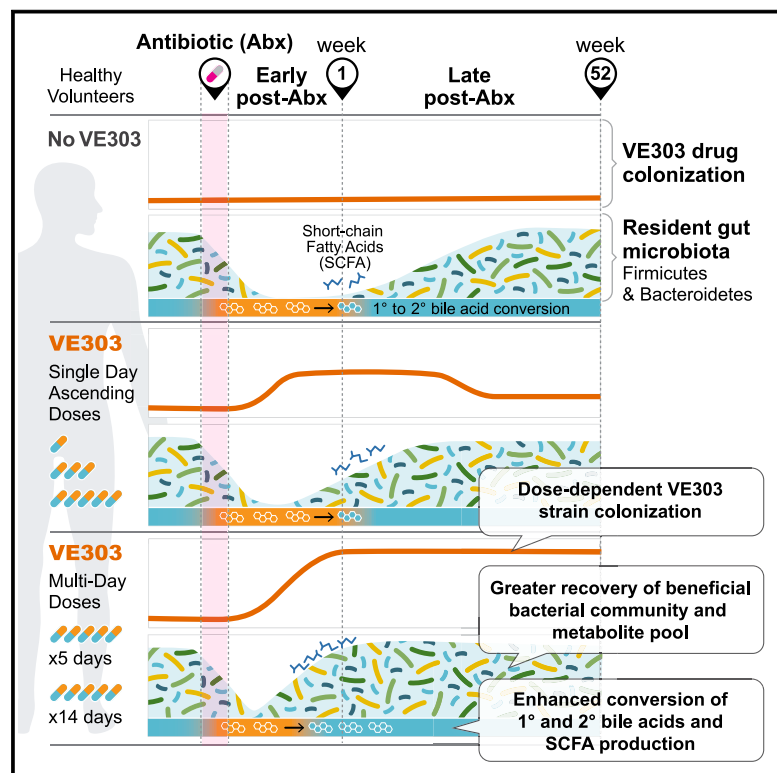
Authors

Melissa Dsouza, Rajita Menon,
Emily Crossette, ..., Bruce Roberts,
Jeremiah Faith, Jason M. Norman

Correspondence

jnorman@vedantabio.com

In brief

Dsouza et al. describe VE303, a live biotherapeutic product under development for the treatment of *C. difficile* infection. A phase 1 study in healthy volunteers found that VE303 is safe and well-tolerated. Dosing VE303 daily for up to 14 days after vancomycin administration promotes rapid and durable VE303 strain colonization.

Highlights

- The VE303 live biotherapeutic product effectively treats *C. difficile* infection in mice

- A phase 1, dose-escalation study shows VE303 to be safe and well-tolerated

- Antibiotic administration and multi-day dosing enables VE303 colonization up to 1 year

- Higher VE303 doses associate with microbiota and metabolite changes

CellPress

Clinical and Translational Report

Colonization of the live biotherapeutic product VE303 and modulation of the microbiota and metabolites in healthy volunteers

Melissa Dsouza,[1,9,10] Rajita Menon,[1,9] Emily Crossette,[1] Shakti K. Bhattarai,[2] Jessica Schneider,[1,11] Yun-Gi Kim,[1,12] Shilpa Reddy,[1] Silvia Caballero,[1] Cintia Felix,[1] Louis Cornacchione,[1] Jared Hendrickson,[1] Andrea R. Watson,[1] Samuel S. Minot,[3] Nick Greenfield,[4] Lisa Schopf,[1,13] Rose Szabady,[1,14] Juan Patarroyo,[1,15] William Smith,[1,11] Pratibha Harrison,[5] Ed J. Kuijper,[6] Ciaran P. Kelly,[7] Bernat Olle,[1] Dmitri Bobilev,[1,16] Jeffrey L. Silber,[1] Vanni Bucci,[2] Bruce Roberts,[1,17] Jeremiah Faith,[8] and Jason M. Norman[1,18,*]

[1]Vedanta Biosciences, Inc., Cambridge, MA 02139, USA
[2]University of Massachusetts Medical School, Department of Microbiology and Physiological Systems, Worcester, MA 01605, USA
[3]Microbiome Research Initiative, Fred Hutchison Cancer Research Center, Seattle, WA, USA
[4]One Codex, Invitae, San Francisco, CA 94103, USA
[5]University of Massachusetts Dartmouth, Bioengineering and Research Core for Microbial Informatics, Dartmouth, MA 02747, USA
[6]Leiden University Medical Center, Leiden, the Netherlands
[7]Beth Israel Deaconess Center, Boston, MA 02215, USA
[8]Icahn School of Medicine at Mount Sinai, New York, NY, USA
[9]These authors contributed equally
[10]Present address: Merck Inc., Cambridge, MA 02141, USA
[11]Present address: Takeda Pharmaceuticals International Co., Cambridge, MA 02139, USA
[12]Present address: Research Center for Drug Discovery, Faculty of Pharmacy, Keio University, Tokyo 105-8512, Japan
[13]Present address: Inflammation and Immunology Research Unit, Pfizer Inc., Cambridge, MA 02139, USA
[14]Present address: Ferring Pharmaceuticals, San Diego, CA, USA
[15]Present address: Novartis Institute for BioMedical Research, Novartis Inc., Cambridge, MA 02139, USA
[16]Present address: Checkmate Pharmaceuticals, Cambridge, MA 02142, USA
[17]Present address: Food Allergy Research and Education, McLean, VA 22102, USA
[18]Lead contact
*Correspondence: jnorman@vedantabio.com
https://doi.org/10.1016/j.chom.2022.03.016

SUMMARY

Manipulation of the gut microbiota via fecal microbiota transplantation (FMT) has shown clinical promise in diseases such as recurrent *Clostridioides difficile* infection (rCDI). However, the variable nature of this approach makes it challenging to describe the relationship between fecal strain colonization, corresponding microbiota changes, and clinical efficacy. Live biotherapeutic products (LBPs) consisting of defined consortia of clonal bacterial isolates have been proposed as an alternative therapeutic class because of their promising preclinical results and safety profile. We describe VE303, an LBP comprising 8 commensal Clostridia strains under development for rCDI, and its early clinical development in healthy volunteers (HVs). In a phase 1a/b study in HVs, VE303 is determined to be safe and well-tolerated at all doses tested. VE303 strains optimally colonize HVs if dosed over multiple days after vancomycin pretreatment. VE303 promotes the establishment of a microbiota community known to provide colonization resistance.

INTRODUCTION

Clinical experience with fecal microbiota transplantation (FMT) indicates that the procedure can be highly effective for the prevention of *C. difficile* infection (CDI) recurrence (Bakken et al., 2011; Kelly et al., 2014; Konturek et al., 2016; Rubin et al., 2013; Youngster et al., 2016), moderately effective for the treatment of ulcerative colitis (Costello et al., 2019; Fuentes et al., 2017; Moayyedi et al., 2015), and is being tested in other conditions, including irritable bowel syndrome (Xu et al., 2019) and obesity (Allegretti et al., 2020). Although FMT has tremendously advanced the clinical application of microbiome science,

it is a challenge to continuously collect healthy donor stool that is screened for potentially transmissible agents with increasingly stringent criteria in response to previous serious adverse events (AEs) (Blaser, 2019; DeFilipp et al., 2019; U.S. Food and Drug Administration, 2020) and a global pandemic of SARS-CoV-2 (Britton et al., 2021; Livanos et al., 2021; Wang et al., 2020).

When applicable to the prevention, treatment, or cure of human diseases, non-vaccine agents composed of live organisms are categorized by the US Food and Drug Administration (FDA) as live biotherapeutic products (LBPs) (Administration US Food and Drug, 2011). Therapeutic LBPs based on defined consortia of isolated microbial strains may provide an alternative

to FMT for some indications (Atarashi et al., 2013, 2015; Furusawa et al., 2013; Kao et al., 2021; Petrof et al., 2013; Tvede and Rask-Madsen, 1989). Defined consortia provide a standardized drug composition with reproducible quality attributes, are amenable to rigorous safety evaluation, and have a clear path to global manufacturing scale and distribution if a specific LBP is demonstrated to be safe and effective in the treatment of a human disease. However, in contrast to FMT, for which numerous studies have provided insights into product stability (Costello et al., 2015), route of administration (Kao et al., 2017; Ramai et al., 2021; Youngster et al., 2016), selective enrichment (McGovern et al., 2021), viable transmission (Aggarwala et al., 2021; Drewes et al., 2019), and durability of colonization (Aggarwala et al., 2021), we know little regarding the parameters that influence the engraftment, durability, and success of LBPs based on defined consortia.

To foster the development of defined consortia as a therapeutic modality for microbiome manipulation to treat human disease, we performed a phase I clinical trial in healthy volunteers (HVs), administering the LBP VE303 with the goals of determining the highest safe and well-tolerated dose and characterizing the effect of dose-escalation and antibiotic pretreatment on LBP colonization for selecting an optimal dose regimen for future clinical studies. The defined consortium VE303, currently in clinical development for the prevention of recurrent *C. difficile* infection (rCDI), is composed of eight commensal strains of Clostridia isolated from healthy donors and selected for the association of strains of these species with successful engraftment and cure of rCDI in a human FMT study as well as their ability to prevent mortality in the cefopera-zone murine model of CDI (Theriot et al., 2011). We found VE303 to be safe and well tolerated at all doses tested, with reliable, durable detection of component strains and robust colonization for up to 1 year after administration. We also found that VE303 administration expedites the establishment of a community enriched for bacteria that are known to provide resistance to *C. difficile* colonization post-vancomycin, particularly when administered on a multiple-dose basis. This enrichment is functionally associated with the recovery of secondary bile acids (BAs) and short-chain fatty acids (SCFAs) in the gut.

RESULTS

Development and characterization of VE303

Recurrent *C. difficile* infection (rCDI) is associated with reduced gut microbiota diversity, including the loss of butyrogenic Firmicutes species (Antharam et al., 2013), increases in the relative abundance (RA) of Proteobacteria, reduced concentrations of SCFA, and changes in the BA pool (Hamilton et al., 2013; Seekatz et al., 2016, 2018). The clinical response to FMT in rCDI patients is associated with the recovery of microbiome diversity and density (Contijoch et al., 2019), the transfer of Clostridium clusters IV and XIVa bacteria (van Nood et al., 2013), and the recovery of metabolites associated with gut health, including SCFA and secondary BAs (Seekatz et al., 2018). To identify a defined bacterial consortium for the treatment of rCDI, we tested several LBP candidates in the cefoperazone mouse model of CDI (Theriot et al., 2011) consisting of consortia of bacterial strains isolated from healthy human donors that varied in

taxonomic complexity and strain number and mostly included Clostridium clusters IV and XIVa bacteria (Collins et al., 1994; Table S1). Diverse LBP candidates (VE308 and VE309) were tested to mimic the taxonomic complexity of whole stool and less complex LBP candidates composed mostly of Clostridium clusters IV and XIVa (VE301 through VE305) were tested based on their association with clinical efficacy in patients with rCDI (Table S1). We employed a "screen for LBP candidates in mice" strategy to identify effective consortia against CDI, as has been used successfully to identify consortia for investigation in inflammatory bowel disease and cancer immunotherapy (Atarashi et al., 2013; Tanoue et al., 2019). In the CDI mouse model, 80% of untreated mice succumbed to the infection before day 4 and treatment with the LBPs VE302, VE304, VE305, and VE309 (LBPs ranging from 3 to 25 strains) did not significantly improve the survival rate (Figure 1A). However, treatment with VE303, an 8-strain consortium, increased the survival rate to 75%, which matched the level of protection exerted by VE308, a more complex, 56-strain consortium (Figure 1A). VE303 is comprised of 5 Clostridium cluster XIVa strains, 2 cluster IV strains, and 1 cluster XVII strain whose species placements (average nucleotide identity [ANI] 95% to 99%) in the genome taxonomy database (GTDB version 89; see method details) include VE303 strain 01 (or VE303-01) *Enterocloster bolteae*, VE303-02 *Anaerotruncus colihominis*, VE303-03 *Sellimonas intestinalis*, VE303-04 Clostridium_Q *symbiosum*, VE303-05 *Blautia* sp001304935, VE303-06 *Dorea longicatena*, VE303-07 *Longicatena innocuum*, and VE303-08 *Flavonifractor* sp000508885 (Table S1). VE303 was efficacious in 5 independent mouse experiments with an average survival rate of 70% (±12%) and increased mouse survival and weight gain to levels comparable with that of FMT (Figures 1B and 1C). While no further characterization was performed on the LBP consortia that failed to protect against CDI *in vivo*, we additionally conducted *in vitro* competition assays investigating the ability of VE303 to directly inhibit *C. difficile*. In these assays, VE303 significantly suppressed the growth of *C. difficile* to levels comparable with that of *Clostridium bifermentans*, a commensal with known anti-*C. difficile* activity (Tvede and Rask-Madsen, 1989; Figure S1A). Strain VE303-06 *Dorea longicatena* was a potent inhibitor of *C. difficile in vitro* (Figure S1B).

To further de-risk advancement of VE303 to human studies, we investigated the prevalence of the VE303 organisms in the stool of a cohort of 74 patients with rCDI who were treated with FMT at Leiden University Medical Center (Nooij et al., 2021). Of these 74 patients, 62 (83.8%) responded to the FMT and did not have a subsequent recurrence up to 8-week post-FMT, whereas 11 of 74 (14.9%) experienced a subsequent recurrence (or relapse) that was confirmed by clinical diagnostic testing for CDI and positive response to antibiotic therapy. One patient (1.4%) likely experienced a recurrence, but this was unconfirmed. Stool samples were collected an average of 15 days before FMT and 31 days after FMT and deep metagenomic sequencing was performed, yielding an average of 40 million reads per sample. Metagenomic sequences were quality filtered and assigned to species using the One Codex software (www.onecodex.com; Minot et al., 2015). We compared the prevalence percentage pre- and post-FMT in subjects that respond to FMT (N = 62) to link treatment efficacy with the observed engraftment success
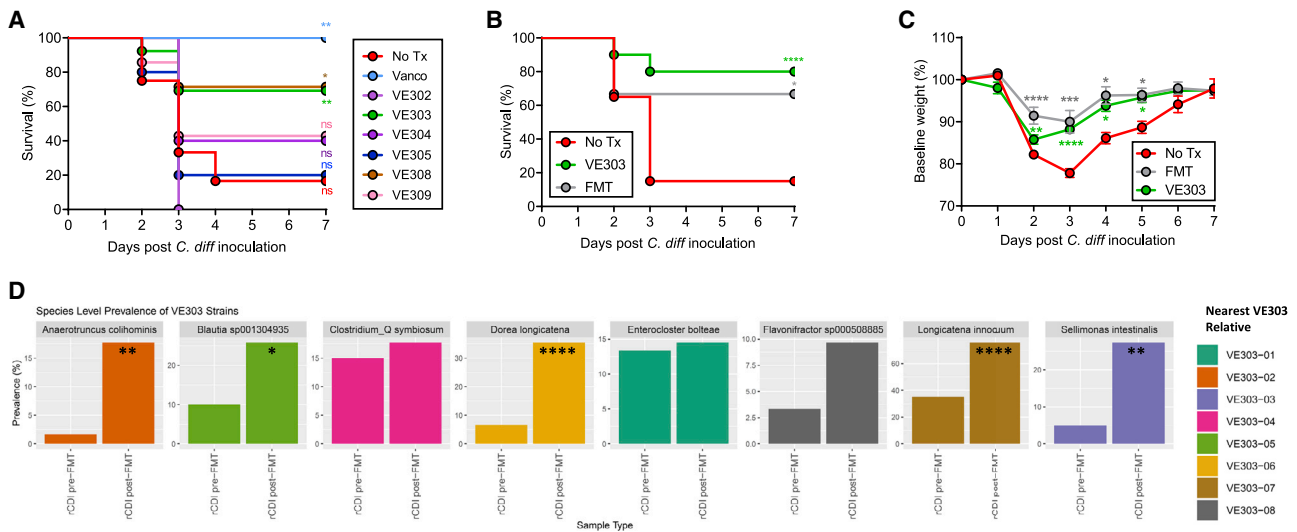
Figure 1. VE303 administration protects against *C. difficile* infection

(A–C) (A and B) Survival and (C) weight of antibiotic-treated mice dosed with any of the following treatments: vancomycin (positive control), bacterial consortia of various sizes and composition, or human FMT 1 day prior to inoculation with *C. difficile*. No Tx groups received either no treatment (A) or were dosed with PBS prior to challenge (B and C, 1 of 2 experiments). ****p < 0.0001; ***p < 0.001; **p ≤ 0.01; *p ≤ 0.05 and ns = not significant compared with the No Tx group. Data shown are mean ± SEM.

(D) VE303 organisms engraft in rCDI patients that responded to FMT treatment at Leiden University Medical Center (Nooij et al., 2021). Five of eight VE303-related species (VE303-02 *Anaerotruncus colihominis*, VE303-03 *Sellimonas intestinalis*, VE303-05 *Blautia* sp001304935, VE303-06 *Dorea longicatena*, and VE303-07 *Longicatena innocuum*) were detected in significantly more responding subjects post-FMT compared with pre-FMT (ZIBR logistic component, adjusted p < 0.05) further supporting the rationale for clinical development of VE303. ****p < 0.0001; ***p < 0.001; **p ≤ 0.01; *p ≤ 0.05.

of individual VE303-related species. Five of eight VE303-related species (VE303-02 *Anaerotruncus colihominis*, VE303-03 *Sellimonas intestinalis*, VE303-05 *Blautia* sp001304935, VE303-06 *Dorea longicatena*, and VE303-07 *Longicatena innocuum*) were significantly increased in prevalence (the percentage of subjects where the species was detected by metagenomics at the indicated time point) in responders post-FMT as compared with pre-FMT (Figure 1D; zero-inflated beta random [ZIBR] logistic component, p < 0.05 after multiple hypothesis correction), further supporting the rationale for clinical development of VE303.

VE303 administration is safe and well-tolerated in healthy volunteers

To advance VE303 into the clinical development pipeline for the treatment of rCDI, we performed a first-in-human phase 1 dose-escalation study to assess the safety and tolerability of VE303 in HV adults with and without vancomycin pretreatment. The phase 1 study was conducted under a US investigational new drug (IND) application, with review by the study site's institutional review board (IRB). Both the US FDA and the IRB reviewed the protocol and informed consent form (ICF) and approved study initiation. The primary objective was to characterize the highest safe and well-tolerated dose regimen of VE303 to guide design of a subsequent phase 2 trial that would evaluate the safety and efficacy of VE303 in the treatment of rCDI. Adverse events (AEs), results of physical examinations, assessment of vital signs, and changes in the clinical laboratory measurements were assessed by a clinical investigator. Secondary objectives included quantifying VE303 engraftment, changes in the intestinal microbiota because of VE303 dosing, and metabolomic changes in the stool.

HVs (N = 39) received either oral vancomycin alone (125 mg 4 times daily [QID] for 5 days in the vancomycin cohort) or vancomycin (125 mg QID for 5 days in cohorts 1, 2, 3, 4, and 5, or 125 mg twice daily [BID] for 3 days in cohort 8) followed by VE303 at ascending doses, or VE303 at the highest dose without vancomycin pretreatment in cohort 6 (total studied dose range was 1.6×10^9 to 1.1×10^{11} colony-forming units [CFUs]) (Table 1). The VE303 drug product (DP) was formulated as a lyophilized consortium containing equal CFU of each individual strain drug substance (DS) into enteric-coated capsules following current good manufacturing practice guidelines (STAR Methods). Both the individual strain DS and the combined DP were highly stable at the recommended storage temperatures (Table S2).

There were no significant differences in the demographic and baseline characteristics among the cohorts (Table 1). Vancomycin was chosen for the pretreatment, as it is the most commonly used first-line therapy for CDI (McDonald et al., 2018), and it has a very-well-understood safety profile since being approved for use by the FDA in 1958 (Levine, 2006). In addition, vancomycin has been used as a pretreatment prior to administration of an LBP for nearly a decade (Villano et al., 2012) and it has been generally well tolerated in this setting.

VE303 was well tolerated in all dose cohorts (Table S3), as determined by the study safety review committee (described in STAR Methods). No serious or severe AEs were reported. Clinical laboratory evaluations, physical examination, and assessment of vital signs did not suggest any abnormalities related to VE303. One or more AEs as defined by the clinical investigator were observed in 76.9% of study subjects, including abdominal distention in 20.5% (8/39), and diarrhea, nausea,

Table 1. VE303 phase 1 dosing summary and demographics

		Vanco (N = 5) n (%)	Cohort 1 (N = 4) n (%)	Cohort 2 (N = 3) n (%)	Cohort 3 (N = 3) n (%)	Cohort 4 (N = 6) n (%)	Cohort 5 (N = 8) n (%)	Cohort 6 (N = 5) n (%)	Cohort 8[a] (N = 5) n (%)	Overall (N = 39) n (%)
Dosing										
Vancomycin		125 mg QID × 5 days	125 mg QID × 5 days	125 mg QID × 5 days	125 mg QID × 5 days	125 mg QID × 5 days	125 mg QID × 5 days	none	125 mg BID × 3 days	–
VE303	daily dose (CFU)	none	1.6×10^9	4.0×10^9	8.0×10^9	8.0×10^9	8.0×10^9	8.0×10^9	$8.0 \times 10^9 \rightarrow 1.6 \times 10^9$	–
	days administered	none	1	1	1	5	14	21	$2 \rightarrow 3$	–
	total dose (CFU)	none	1.6×10^9	4.0×10^9	8.0×10^9	4.0×10^{10}	1.1×10^{11}	1.7×10^{11}	2.1×10^{10}	–
Characteristic	**Statistic**									
Age (years)	N	5	4	3	3	6	8	5	5	39
	mean (SD)	38.2 (12.07)	35.5 (8.35)	51.7 (5.13)	45.3 (14.57)	37.0 (11.47)	34.5 (9.65)	41.2 (12.72)	39.0 (11.25)	39.1 (11.00)
	Median	34.0	33.5	53.0	47.0	32.0	31.0	43.0	37.0	36.0
	min, max	27, 53	28, 47	46, 56	30, 59	26, 52	25, 53	25, 56	27, 53	25, 59
Gender, n (%)	Female	4 (80.0%)	2 (50.0%)	1 (33.3%)	1 (33.3%)	1 (16.7%)	3 (37.5%)	2 (40.0%)	0	14 (35.9%)
	Male	1 (20.0%)	2 (50.0%)	2 (66.7%)	2 (66.7%)	5 (83.3%)	5 (62.5%)	3 (60.0%)	5 (100.0%)	25 (64.1%)
Ethnicity, n (%)	hispanic or latino	1 (20.0%)	1 (25.0%)	1 (33.3%)	0	0	1 (12.5%)	0	1 (20.0%)	5 (12.8%)
	not hispanic or latino	4 (80.0%)	3 (75.0%)	2 (66.7%)	3 (100.0%)	6 (100.0%)	7 (87.5%)	5 (100.0%)	4 (80.0%)	34 (87.2%)
Race, n (%)	Black or african american	4 (80.0%)	2 (50.0%)	1 (33.3%)	2 (66.7%)	6 (100.0%)	6 (75.0%)	1 (20.0%)	3 (60.0%)	25 (64.1%)
	mixed/other	0	1 (25.0%)	0	0	0	0	0	0	1 (2.6%)
	White	1 (20.0%)	1 (25.0%)	2 (66.7%)	1 (33.3%)	0	2 (25.0%)	4 (80.0%)	2 (40.0%)	13 (33.3%)
Height (cm)	N	5	4	3	3	6	8	5	5	39
	mean (SD)	162.8 (14.96)	164.5 (13.70)	173.7 (10.41)	172.3 (3.21)	175.2 (6.68)	171.1 (7.89)	170.4 (11.39)	172.4 (8.67)	170.3 (10.01)
	Median	158.0	168.0	177.0	171.0	173.0	172.5	173.0	174.1	171.0
	min, max	152, 189	145, 177	162, 182	170, 176	169, 186	158, 180	151, 180	163, 185	145, 189
Weight (kg)	N	5	4	3	3	6	8	5	5	39
	mean (SD)	72.8 (20.28)	74.9 (17.13)	84.5 (12.41)	81.3 (7.76)	72.6 (13.26)	76.1 (12.03)	80.9 (14.89)	75.3 (6.42)	76.6 (13.01)
	Median	69.2	73.8	81.3	81.7	74.9	78.4	86.1	77.2	77.2
	min, max	57, 106	58, 94	74, 98	73, 89	57, 86	57, 90	60, 97	68, 82	57, 106
BMI (kg/m^2)	N	5	4	3	3	6	8	5	5	39
	mean (SD)	27.1 (3.54)	27.6 (4.59)	27.9 (1.86)	27.4 (1.97)	23.6 (3.65)	25.9 (2.92)	27.6 (2.57)	25.5 (3.42)	26.3 (3.27)
	Median	29.1	29.8	28.1	28.3	23.8	25.5	28.6	24.0	26.5
	min, max	23, 30	21, 30	26, 30	25, 29	20, 29	22, 30	24, 30	23, 30	20, 30

[a]Subjects enrolled in cohort 8 were given a shorter vancomycin regimen (125 mg BID × 3 days) compared with cohorts 1 through 5, followed by a tapered VE303 dosing schedule.
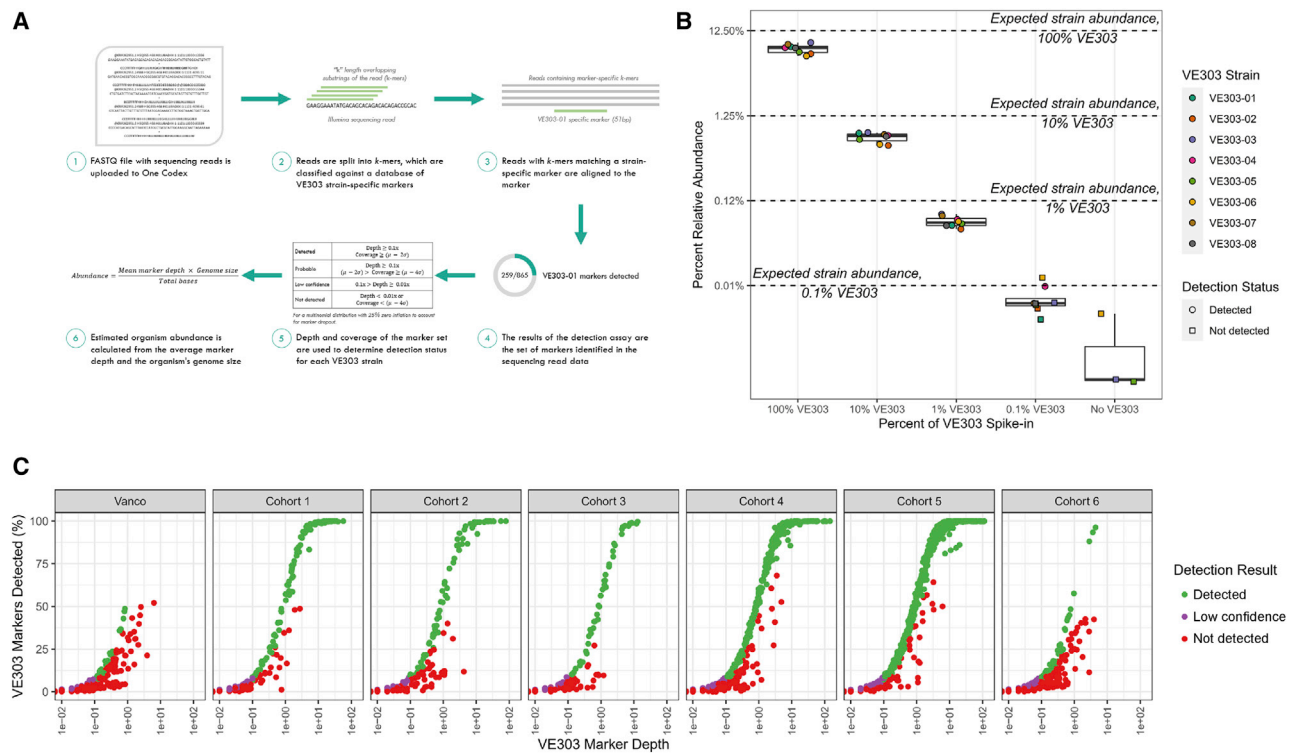
Figure 2. Marker-based bioinformatics assay for sensitive and specific detection of VE303 organisms

(A) Shotgun metagenomic sequences are run through a bioinformatic assay based on the detection of curated k-mer sets unique to each VE303 strain.
(B) Detection accuracy was validated using human stool DNA spiked with varying amounts of VE303 (0%, 0.1%, 1%, and 10% of total DNA) before metagenomic sequence analysis. The mass of each strain's DNA is the same across all spike ins (i.e., at 1% total VE303, each strain's DNA is 0.125% of the total DNA). Additionally, one sample that comprised equal proportions of all 8 VE303 strain DNAs (100% VE303) was also sequenced. Individual strains are recovered lower than expected relative abundance with a limit of detection of 0.0125% abundance per strain: circular points indicate high-confidence detection and square points indicate spurious or no-detection. The box and whisker plots indicate the median relative abundance (±interquartile range and 1.5x interquartile range).
(C) Confidence in detection status based on marker depth and number of markers detected in HV stool samples. Assay detection status is determined based on agreement within two standard deviations of the expected k-mer coverage-depth distribution for shotgun sequencing data (Green, detected; red, not detected, purple, low confidence; see STAR Methods).

headache, and increased lipase each in 12.8% (5/39). No clinically meaningful dose- or duration-related trends were observed concerning AE incidence (Table S3). All AEs determined to be VE303 related were mild (Grade 1) and transient, and most cases of abdominal distention and nausea were attributed by the clinical investigator to be related to the oral vancomycin pretreatment rather than to VE303. The overall AE reporting rates were 58.8% during the vancomycin period and 60.6% during the VE303 period. Although mean increases or decreases from baseline were observed across hematology, chemistry, and urinalysis parameters across cohorts after administration of VE303, no apparent treatment-specific trends were noted; most abnormal laboratory findings were Grade 1. Sporadic Grade 2 or higher abnormalities were reported for glucose, blood urea nitrogen, creatinine, alanine aminotransferase, creatine phosphokinase, amylase, lipase, and hemoglobin.

The results with respect to the secondary objectives are presented here for 32 of the VE303 recipients, as one subject in cohort 1 withdrew from the study and one subject in cohort 5 was excluded due to non-compliance. All cohort 8 subjects (n = 5) were excluded due to the unique dosing regimens for

both vancomycin (lower daily dose and number of days) and VE303 (variable daily dose) compared with the other cohorts, confounding the attribution of subsequent strain colonization and community ecological shifts to either. As expected, given the generally benign safety profile of far more complex consortia from well-screened FMT donors, the overall safety profile of VE303 in this trial was acceptable and sufficient for advancement to additional clinical testing in the context of rCDI in phase 2.

VE303 strains rapidly and durably colonize human volunteers

To measure the colonization of VE303, we used an *in vitro* validated, strain-level bacterial detection method that enables the differentiation of VE303 consortium member strains from highly related, endogenous taxa (Figure 2; described in method details). This method, which has a similar objective as other strain tracking algorithms (Aggarwala et al., 2021; Ferretti et al., 2018; Korpela et al., 2018; Nayfach and Pollard, 2016; Olm et al., 2021), detects VE303 strains in stool metagenomes utilizing unique 50-bp genomic markers spanning the length of the VE303 strain genomes (Table S4). The RA of each strain

was calculated as the total marker depth per strain (the ratio of reads matching any marker to the total number of markers) divided by the total bases and multiplied by the genome size. Confidence in the detection of VE303 strains in each patient sample was determined by assessing the distribution of marker depth (the fraction of sequenced reads matching any marker) to marker coverage (the fraction of markers with ≥1 matching read) (Figure 2C). A strain was considered "Detected" when the mean marker depth exceeded 0.1×, and the coverage of markers detected was within two standard deviations of the mean expected from a multinomial k-mer coverage-depth distribution for shotgun sequencing data (with 25% zero inflation to account for marker dropout) (green circles, Figure 2C). The threshold of 0.1× was chosen to ensure that genomic data were recovered from each organism at a level sufficient to distinguish genomic signal from near neighbors; strains detected at a marker depth between 0.01× and 0.1× were considered "low-confidence" hits. In contrast, samples with a high (>0.1×) VE303 strain marker depth attributed to a very small fraction of the unique marker set may signal non-specific detection, partial marker overlap with similar strains, or other artifacts. Under the detection scheme, such samples fell outside the specified confidence bands (red circles, Figure 2C) and were assigned a detection status of "not detected." Overall, the set thresholds specify the extent of acceptable deviation from the region of the coverage-depth distribution where VE303 strains are reliably detected, determining "detected," "not detected," or "low confidence" strain detection status in patient samples (see method details).

To validate the strain detection method, we spiked VE303 strain genomic DNA (at 0%, 0.1%, 1%, 10%, and 100% total spike-in, with equal amounts of DNA per strain) into healthy donor stool DNA before metagenomic sequence analysis (Figure 2B). We determined that the algorithm can sensitively detect most strains above a per-strain RA of 0.0125%. For all spike-in amounts, the median observed RA of each strain was 37%–45% below the expected RA (Figure 2B), suggesting that the assay is sensitive but may underestimate the RA for each strain. Additional *in silico* and *in vitro* validation was performed as described in the STAR Methods details.

Stool samples were collected longitudinally from each subject to determine the baseline microbiome composition, the composition after vancomycin administration, and the prevalence and RA of VE303 strains after LBP administration by metagenomic sequencing (Figure S2). Each stool sample was sequenced at a target depth of >4 Gb on the Illumina NextSeq platform (an average of $4.4 \times 10^7 \pm 1.1 \times 10^7$ reads). VE303 strains were detected at less than 0.1% RA in some subjects at baseline time points and in the vancomycin cohort (Figure S3). These detection events categorized as "detected" in the vancomycin cohort were just above the "low-confidence" threshold and are likely close relatives of the VE303 strains, with partial overlap to the strain marker panel.

In subjects dosed with VE303 following vancomycin (cohorts 1 to 5), the VE303 component strains were detected within the first 24–48 h after beginning VE303 administration (Figure 3). After a single dose of VE303 (cohorts 1, 2, and 3), a median of 37.5%–75% of the strains were detected 2 days later (study day 8) (Figure 3A). There was considerable variability in the strain

detection among subjects receiving a single dose of VE303, ranging from 1 to 8 strains at 48 h after dosing (Figures 3A and S3B). The number of VE303 strains detected in the single-ascending-dose cohorts (cohorts 1, 2, and 3) was not improved with an increase in CFUs administered (Kruskal-Wallis, p = 0.87).

Multiple days of VE303 administration after a short course of vancomycin (cohorts 4 and 5) resulted in more robust and consistent strain detection than did single-day administration. Two days after the start of VE303 administration (study day 8), the median percentage of strains detected in the multi-day cohorts 4 and 5 were comparable to the single-day cohorts 1, 2, and 3. However, the median percentage of VE303 strains detected per subject 1 week after starting VE303 dosing (day 14) was 100% for both multi-day cohorts (Figure 3A), peaking at day 14. In 3 of 6 subjects in cohort 4 and all 7 subjects analyzed in cohort 5, all 8 VE303 strains were detected at multiple time points (Figures 3C and S3C).

The total RA of VE303 strains was also highest in cohorts 4 and 5, suggesting that multiple days of LBP administration facilitates colonization (Figure 3B). The total VE303 RA peaked between 1 and 2 weeks after starting VE303, reaching a median total RA of 2.6% and 7.0% at day 14 for cohorts 4 and 5, respectively. VE303 strain colonization steadily declined after stopping VE303 administration. Strain detection and RA remained high through week 12 (11 and 10 weeks after stopping VE303 in cohorts 4 and 5, respectively), with a median number of strains detected of at least 5 and a total RA greater than 1%. We observed some inter-individual variability in the detection and RA of VE303 strains, especially after week 12, but the strains were still present over the entire follow-up period, to a total RA of 0.5% and 0.1% at 1 year for cohorts 4 and 5, respectively. The poor overall colonization in cohort 6 subjects who were dosed with VE303 for multiple days but not pre-treated with vancomycin suggests that, at least for healthy individuals, depletion of the endogenous gut microbiome is critically important for LBP colonization at the doses tested in this study (Figures 3A and 3B).

To characterize the dynamics of acute VE303 strain colonization and effects of multiple- versus single-day dosing, we fit logistic curves to the absolute abundance (or concentration) of VE303 strains (ng strain/mg stool) measured in stool over 60 days from the start of vancomycin treatment. We then calculated the area under the concentration-time curve (AUC in ng strain/mg stool days) (Isabella et al., 2018) up to day 20 (Figure 3E). In Figure S3E, we illustrate an example of a concentration-time curve (subject 171, cohort 5, VE303 strain 8) used to quantify the AUC. A comparison of single-dose (cohorts 1, 2, and 3) and multiple-dose (cohorts 4 and 5) cohorts administered vancomycin revealed an aggregate total dose-dependent increase in the median AUC, which increased from 0.43 for the combined single-dose cohorts to 0.72 for cohort 4 (Dunn pairwise post hoc test p = 0.051) and 1.3 for cohort 5 (Dunn pairwise post hoc test, p < 0.001). In cohorts 4 and 5, we observed significant trends in the individual strain AUCs, with strains VE303-02 and VE303-03 having the lowest median AUCs and strains VE303-01 and VE303-08 having the highest median AUCs. These differences were significant (Dunn's pairwise post hoc test p < 0.005). The median AUC for cohort 6 (no vancomycin administration) was below 0.001, over 1,000-fold below the
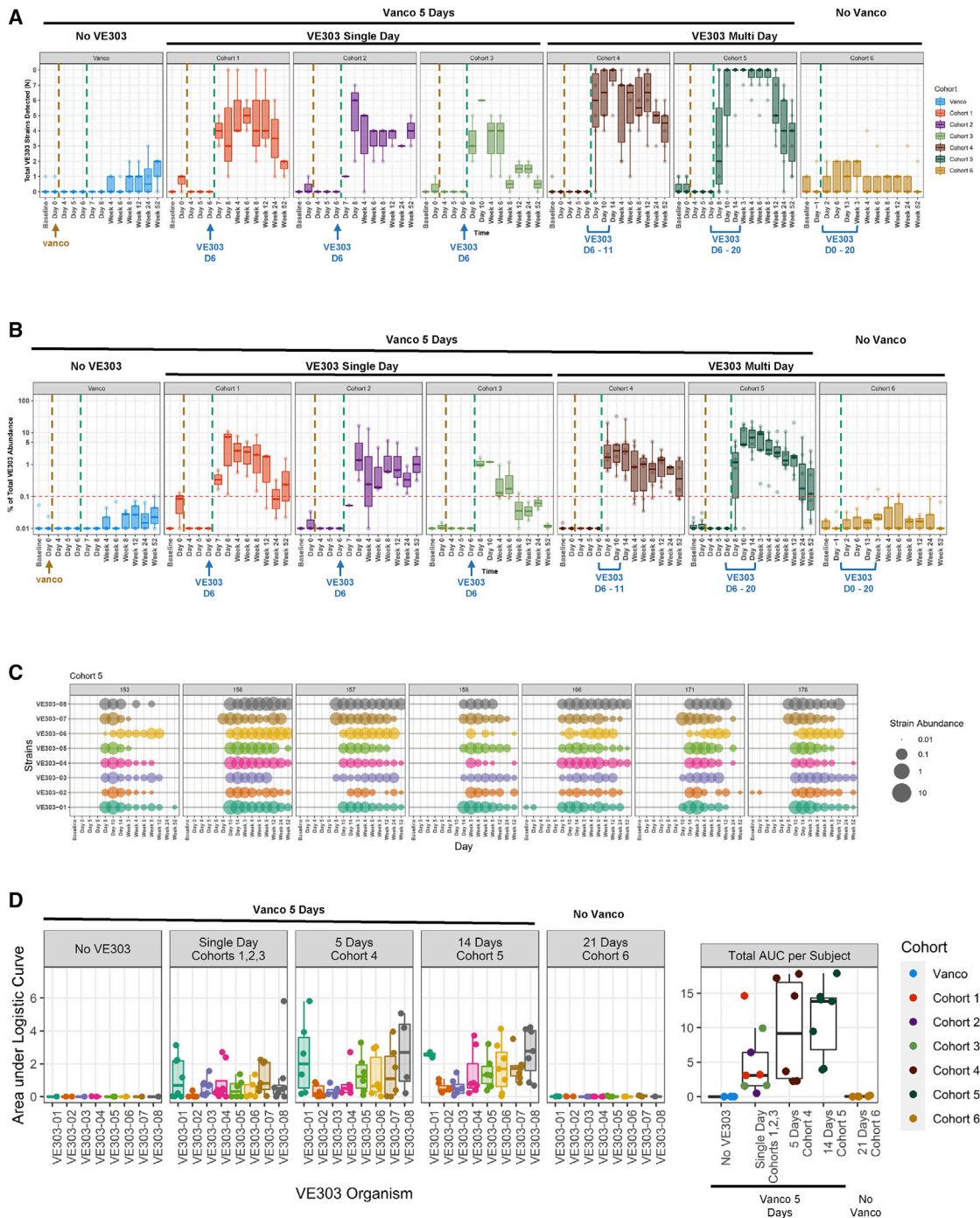
Figure 3. Colonization of VE303 strains in healthy volunteers

(A and B) Box and whisker plots indicating (A) the total number of VE303 strains detected and (B) the total VE303 strain relative abundance at the indicated collection time points. The median (±interquartile range and 95% confidence) are plotted for each. The days of vancomycin and VE303 LBP administration are indicated for each cohort and correspond to Table 1 and Figure S2. The dashed brown line indicates the start of vancomycin administration. The dashed teal line indicates the start of VE303 administration and/or the start of the recovery from vancomycin.

(C) Individual VE303 strains colonize at high prevalence and abundance across all subjects within cohort 5. Circle size indicates the log relative abundance values for each detected strain. VE303 strain detection across all cohorts over time is shown in Figure S3.

(D) A logistic growth model was used to estimate area under the logistic curve (AUC) as a measure of overall colonization per strain (see STAR Methods). Cohorts 4 and 5 show highest strain-wise and total colonization within VE303-dosed cohorts, while strains are largely absent from cohort 6 and the vancomycin-only cohort. Within cohorts 4 and 5, VE303-01 and VE303-08 AUC values significantly higher than VE303-02 and VE303-03 (Dunn pairwise post hoc tests. VE303-01 to VE303-02, $p = 0.002$; VE303-01 to VE303-03, $p = 0.002$; VE303-02 to VE303-08, $p = 0.005$; VE303-03 to VE303-08, $p = 0.004$). The box and whisker plots indicate the median AUC (±interquartile range and 1.5× interquartile range).

median of cohort 5, thus providing further evidence that vancomycin was required to see robust colonization in HVs. Overall, these data demonstrate that dosing for multiple days after a short vancomycin course leads to robust, durable colonization of the human gut with VE303 strains.

VE303 administration promotes a microbiota community known to resist enteric pathogen colonization

The metagenomics data collected pre- and post-vancomycin administration were used to assess the dynamics of the stool microbiota in HVs and the effect of VE303 administration on the community dynamics following antibiotic-induced perturbations. In these analyses, we defined the following sample groupings: baseline (samples collected at screening or study day 0), vanco (samples collected after completion of vancomycin but before VE303 or study day 5 and day 6), early recovery (samples collected up to 1 week after stopping vancomycin ±VE303), and late recovery (samples collected more than 1 week after stopping vancomycin ±VE303). As expected, the baseline microbiota had high total absolute abundance (or bacterial density as ng bacterial DNA per mg stool) and diversity (Figures S4A and S4C) and was dominated by Bacteroidetes and Firmicutes species (Figure S4B). Vancomycin administration resulted in an average 16.6-fold reduction in bacterial density per subject (range 2- to 48-fold) (Figure S4A), an average of 2.3-fold reduction in Shannon diversity per subject (range 1- to 5-fold) (Figure S4C), and a shift in the composition of the microbiota, indicated by reduced density of Bacteroidetes and Firmicutes and increased Proteobacteria (Figure S4B). Species richness recovered to pre-vancomycin levels, defined as a non-significant difference by linear mixed effects (LMEs) modeling, as early as week 4 post-VE303 dosing in cohorts 1 and 3. Pre-vancomycin species richness was recovered at week 6 and week 24 in cohorts 2 and 5, respectively, and never recovered in cohort 4 within the 1 year follow-up period (Figure 4A; Table S4). The beta diversity (Aitchison's distance) revealed that vancomycin administration significantly altered the microbiota community from baseline across all cohorts (permutational multivariate analysis of variance (PERMANOVA) p < 0.05), and the diversity remained altered compared to baseline up to 1 year post-vancomycin (Figure S4D; Table S5). These long-term effects of vancomycin administration are consistent with previous reports demonstrating the loss of species after vancomycin administration and the ability to introduce new species post-antibiotics (Henn et al., 2021; Palleja et al., 2018). No significant diversity or bacterial density changes were observed in cohort 6, in the absence of vancomycin (p > 0.05) (Figures 4A and S4).

We investigated the taxonomic groups contributing to the observed ecological shifts in the patients' gut microbiota. In particular, we identified native Clostridia displaced by VE303 in recipients: species that remained low in abundance compared with baseline after stopping vancomycin and were negatively associated with VE303 colonization (Figure S4E; STAR Methods). Notably, displaced taxa included near relatives of VE303 organisms, including several *Blautia spp.* (species relatives of VE303-05) and *Erysipelotrichaceae bacterium 21_3* (GTDB species Clostridium_AQ *innocuum*, a taxonomic relative of VE303-07), suggesting the exclusion of endogenous species functionally related to VE303 species due to the successful colonization of the

latter. Specifically, the endogenous butyrate producers *Intestinibacter butyriciproducens* and *Faecalibacterium prausnitzii* are displaced by VE303; however, several VE303 strains are predicted to functionally replace this phenotype, as they produce butyrate *in vitro* (Figure S1E; VE303-02 *Anaerotruncus colihominis*, VE303-04 Clostridium_Q *symbiosum*, VE303-07 *Longicatena innocuum*, and VE303-08 *Flavonifractor* sp000508885). Furthermore, strains VE303-07 and VE303-08 are consistently the highest colonizers within the consortium (Figure 2). The replacement of endogenous SCFA-producing bacteria by VE303, in particular with high-colonizing butyrate-producer strains VE303-07 and VE303-08, suggests the maintenance of functional SCFA metabolism within the recipients.

To characterize overall taxonomic changes and evaluate the VE303 dose response in this study, we calculated the ratio of bacterial classes that were reduced by vancomycin (Bacteroidia, Clostridia, Actinobacteria, Verrucomicrobiae, and Coriobacteriia) to the bacterial classes that were increased in abundance by vancomycin and are often described as being associated with disease (Gammaproteobacteria, Alphaproteobacteria, Bacilli, Desulfovibrionia, Fusobacteria, and Negativicutes) (Blount et al., 2018). The ratio of total RA of these taxa or "post-vancomycin microbiota recovery index" (pVMRI) was rapidly reduced by 1,000-fold after vancomycin and required ∼1 month to return to baseline levels in cohort 1, 2, and vancomycin-only subjects (Figure 4B). In cohorts administered higher VE303 doses (cohorts 3, 4, and 5) the pVMRI significantly increased within 1 week of starting VE303 compared with vancomycin only (Figures 4B and 4C; Table S5, LME p < 0.01).

The expedited return to near baseline pVMRI levels with multiple doses of VE303 was characterized by significant changes in microbes at multiple taxonomic levels. This was most apparent in cohort 4 subjects when compared with vancomycin-only subjects. In the 1-week post-vancomycin window, multiple days of VE303 administration was associated with a significant (LME p < 0.05) increase in genera within the class Clostridia, including non-VE303 genera (Figure 4D). This coincided with a significant (LME p < 0.05) reduction in Klebsiella_A species and multiple genera within the family *Lactobacillaceae* (assignments according to GTDB). In cohort 5 subjects, genera of *Lactobacillaceae* and Klebsiella_A species were significantly (LME p < 0.05) reduced and a significant increase in Eubacterium_D species was observed within the 1-week post-vancomycin window when compared with vancomycin-only subjects (Figure 4D; Table S6). There were no significant changes in the overall taxonomic composition (Figures 4B and 4C) or in specific taxa (Figure 4D) in subjects administered VE303 without vancomycin (cohort 6).

In patients who experience an episode of *C. difficile*, the risk for developing a subsequent CDI recurrence is between 7- and 10-fold higher during antibiotic therapy and in the first month after cessation of treatment, compared with the period between 1 and 3 months after antibiotic exposure (Hensgens et al., 2012). The risk for developing CDI is coincident with antibiotic-induced dysbiosis that can persist for several weeks or even months upon completion of treatment. As an intact microbiota provides colonization resistance against enteric pathogens, minimizing the time spent in a perturbed post-antibiotic microbiota state by administering VE303 merits exploration as a strategy to lower rates of rCDI.
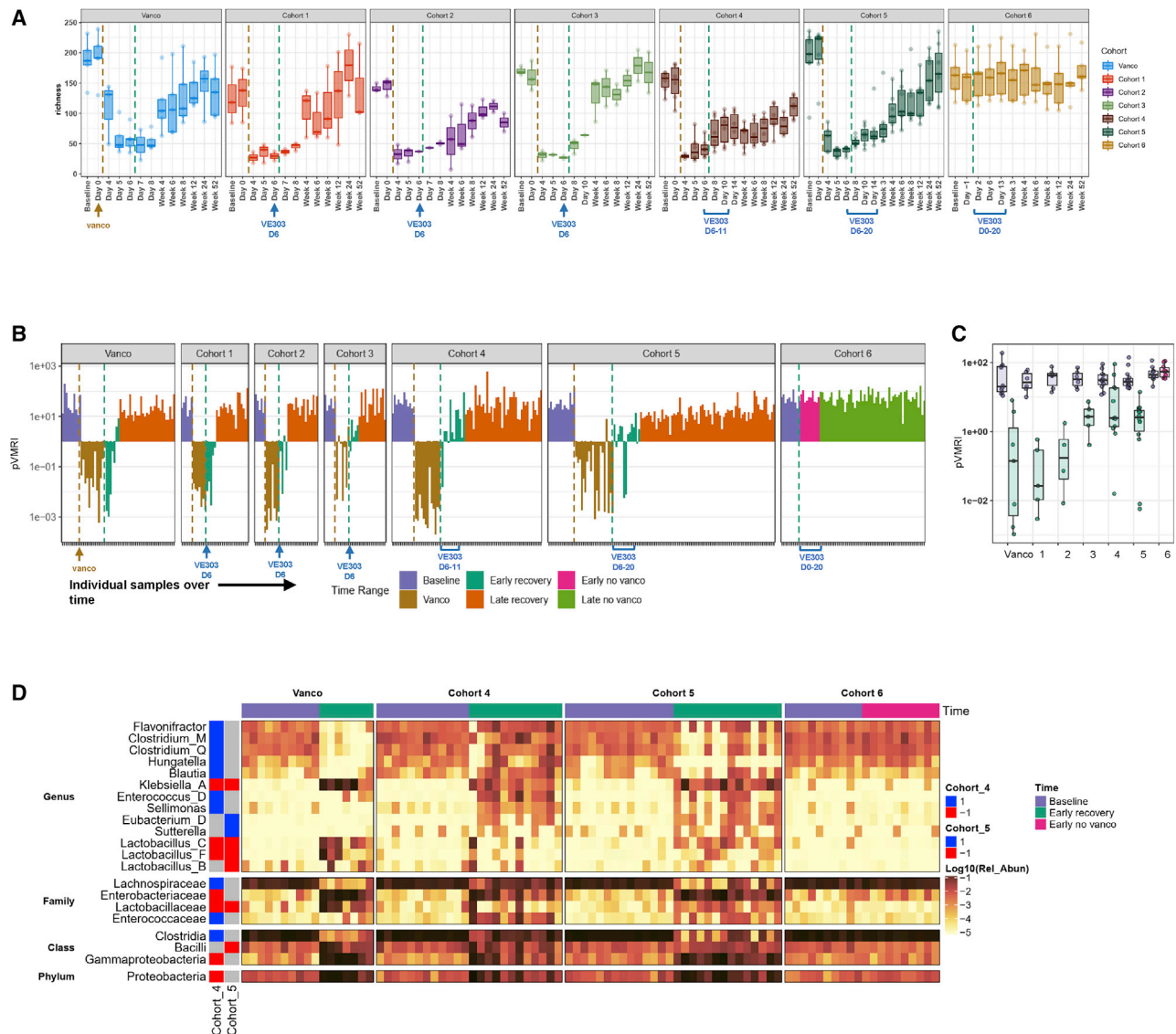
Figure 4. Microbiota dynamics with vancomycin and VE303

(A) The species richness of the stool microbiome over time for each cohort. The box and whisker plots depict the median, interquartile range, and 95% confidence intervals.

(B) Bar plots of the post-vancomycin microbiota recovery index (pVMRI; see Equation 2) colored according to time point where "baseline" corresponds to the starting community; "vanco" equals days 4–6 of the study; "early recovery" equals days 7–13 of the study (or 1-week post-vancomycin with or without VE303); "late recovery" equals study days greater than or equal to 14; "early no vanco" equals study days 1–7 (or 1-week post-VE303 for cohort 6 only); and "Late no vanco" equals study days greater than or equal to 8 for cohort 6 only. The pVMRI is plotted on a log 10 scale. The brown dashed line indicates the start of vancomycin administration and the teal dashed line indicates the start of the VE303 administration period.

(C) Box and whisker plot indicating the microbiota response at increasing VE303 doses measured by the pVMRI during the "baseline," "early recovery," and "early no vanco" time points across all cohorts. The plot depicts the median pVMRI, interquartile range, and 95% confidence intervals.

(D) Heatmap depicting members of the microbiota that were significantly enhanced in VE303-dosed cohorts 4 and 5 compared with vancomycin-only within 1 week of dosing (p < 0.05). Row annotations represent positive/negative enrichment of each taxon by cohort. Taxa marked in red are reduced and those marked with blue are enriched in VE303-dosed cohorts. All taxa marked in gray were not significantly altered by VE303 dosing.

Vancomycin disrupts the gut metabolite pool and VE303 colonization is associated with increased concentrations of secondary BAs and short-chain fatty acids

BAs play an important role in establishing colonization resistance against CDI. Whereas a subset of primary BAs trigger *C. difficile*

spore germination and permit outgrowth of vegetative cells (Sorg and Sonenshein, 2008) and are elevated in patients with CDI (Foley et al., 2019; Seekatz et al., 2018; Winston and Theriot, 2019), secondary BAs abate spore germination and growth (Chen et al., 2019; Foley et al., 2019; Kang et al., 2019; Palmieri et al., 2018; Seekatz et al., 2018; Thanissery et al., 2017).
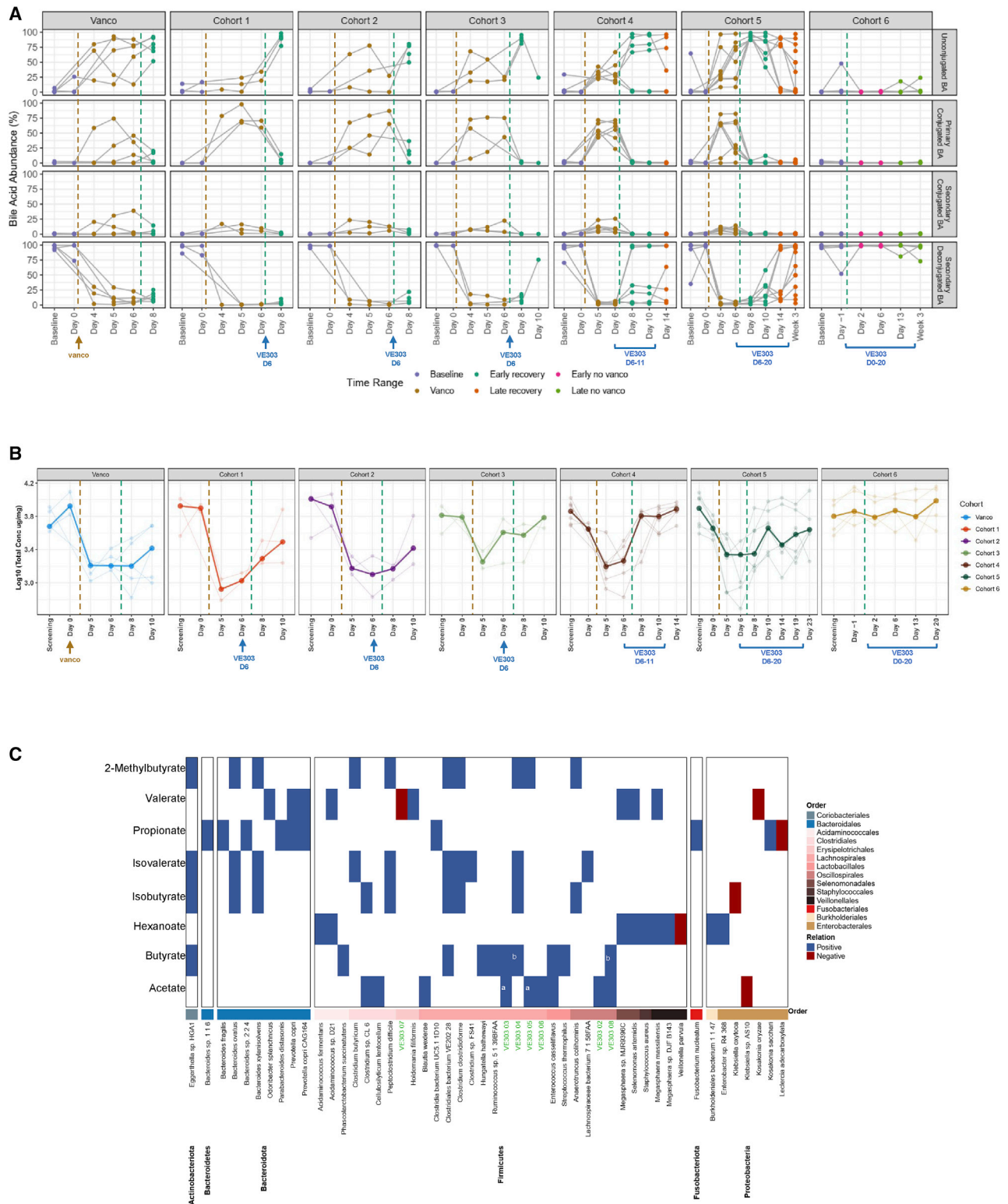
Figure 5. Bile acid and short-chain fatty acid dynamics with vancomycin and VE303

(A) Bile acid concentrations, particularly secondary deconjugated BAs, are impacted by vancomycin pretreatment and return to baseline with VE303 administration. Line plots indicate total BA concentrations for primary unconjugated, primary conjugated, secondary conjugated, and secondary deconjugated bile acids for individual subjects in each cohort. Points are colored according to time point where "Baseline" corresponds to the starting community; "vanco" equals days 4–6 of the study; "early recovery" equals days 7–13 of the study (or 1-week post-vancomycin with or without VE303); "late recovery" equals study days greater

(legend continued on next page)

Clostridium clusters IV and XIVa species are involved in the conversion of primary BAs to secondary BAs; higher levels of secondary BAs in the gut are an established function of a gut microbiota associated with resistance to pathogens (Allain et al., 2017; Thanissery et al., 2017). BA concentrations were measured in the stool pre- and post-vancomycin administration to evaluate their dynamics in HVs and associations with VE303 administration. At baseline, secondary deconjugated BAs including deoxycholic acid (DCA), lithocholic acid (LCA), and ursodeoxycholic acid (UDCA) made up the largest proportion of BAs in the stool in all cohorts (Figures 5A and S5A). Likewise in all cohorts, treatment with vancomycin led to a significant (LME, p < 0.01) reduction in the secondary deconjugated BAs LCA and DCA, and an increase in the proportion of primary BAs including cholic acid (CA) and chenodeoxycholic acid (CDCA) and their glycine and taurine conjugated forms (primary conjugated BAs). 2 days following vancomycin administration, we observed elevation of primary BAs and a reduction in secondary BAs in subjects only receiving vancomycin. In subjects receiving multiple doses of VE303 (cohorts 4 and 5), we observed an increase by day 10 in the levels of deconjugated secondary BAs by 15- to 44-fold and a decrease in the levels of primary BAs by 46- to 122-fold (Figures 5A and S5A). Most notably, we observed a significant association between the total engraftment of VE303 and both the increase in LCA and DCA and the decrease in primary BAs (LME p < 0.01) (Table S7).

We used random forest regression (RFR) to decouple the effects of VE303 strains and resident bacterial species on BA concentrations after vancomycin administration. RFR indicated that VE303 strains were associated with the observed increase in secondary BAs (Table S7), particularly UDCA, which is the product of an epimerization reaction of CDCA and is known to inhibit *C. difficile* (Palmieri et al., 2018; Weingarden et al., 2016). Resident commensal species including *Eggerthella* sp., *Phascolarctobacterium* sp., *Bacteroides dorei*, *Odoribacter splanchnicus*, *Clostridum* spp., and *Eubacterium limosum* were important for the expedited recovery of DCA and LCA in the presence of VE303. These strains are hypothesized to play a significant role in BA metabolism (Heinken et al., 2019).

The conversion of primary BAs to secondary BAs involves a series of hydroxylation, deconjugation, and epimerization reactions (Foley et al., 2019; Winston and Theriot, 2019). We explored the potential of the VE303 strains to contribute to secondary BA production by mining their genomes for the presence of genes that carry out these transformations: bile salt hydrolase (BSH), hydroxysteroid dehydrogenase (HSDH), and *bai* operon genes. All VE303 strains were found to have one or more BSH genes (Figure S1D), which encode enzymes that carry out the first step in deconjuga-

tion of the primary BAs CA and CDCA (Foley et al., 2019). Four of the eight strains (VE303-01, VE303-04, VE303-06, and VE303-08) were found to encode protein sequences (similarity > 94%) for 7a-, 3a/3b-HSDH enzymes, which are involved in the epimerization reaction of CDCA to UDCA (Winston and Theriot, 2019), which is consistent with the observed VE303 associations in the phase 1 study. Coding regions in VE303-03, VE303-05, and VE303-07 also matched protein sequences for 7a-, 3a/3b-HSDH enzymes but with lower sequence identity (65%–78%). The VE303 strains did not encode the *bai* operon genes. In summary, our analysis indicates that VE303 organisms encode some but not all of the necessary biochemical pathways required for secondary BA production. Taken together, these data suggest the VE303 consortium strains may act in concert with other intestinal bacteria to carry out the conversion of primary BAs to secondary BAs.

Microbiome-produced SCFAs are known to positively affect host physiology in the gut by promoting gut barrier function and in peripheral tissues by providing anti-inflammatory, antitumorigenic, and antimicrobial functions (Bishehsari et al., 2018; Cait et al., 2018; Donohoe et al., 2014; Fachi et al., 2019; Kim et al., 2018; Luethy et al., 2017; Zhao et al., 2018). SCFAs are also correlated with colonization resistance against *C. difficile* (Theriot et al., 2014) and protect against *C. difficile*-induced colitis (Fachi et al., 2019). Reduction in SCFA levels and the abundance of SCFA-producing bacteria have been associated with several autoimmune, allergic, and metabolic diseases (Aitoro et al., 2017; Belkaid and Hand, 2014; Geva-Zatorsky et al., 2017; Manfredo Vieira et al., 2018; Sze and Schloss, 2016; Tan et al., 2016; Zou et al., 2018). SCFA concentrations were measured in the stool pre- and post-vancomycin administration to evaluate their dynamics in HVs and their associations with VE303 administration. Vancomycin resulted in a ~5-fold reduction in the total SCFA pool (Figure 5B) and a significant reduction in acetate, butyrate, and propionate across all cohorts (LME p < 0.05) (Figure S5B; Table S7). The SCFA levels remained low in vancomycin-only subjects for 2–4 days after stopping the antibiotic, but an increase in the total SCFAs (Figure 5B) and significant increases in butyrate, acetate, isobutyrate, 2-methylbutyrate, isovalerate, and propionate were observed in subjects given multiple days of VE303 during this early period after receiving antibiotics (LME p < 0.05) (Figure S5B; Table S7).

RFR analysis identified six VE303 strains as among the top 20 (of 317) most important taxa that were significantly associated with increased SCFAs (Figure 5C). Along with resident species, VE303 strains were significantly associated with increases in the levels of acetate, butyrate, isobutyrate, methylbutyrate, and isovalerate; commensal Bacteroidetes species were significantly associated with the increase in propionate (p < 0.05)

than or equal to 14; "early no vanco" equals study days 1–7 (or 1-week post-VE303 for cohort 6 only); and "Late no vanco" equals study days greater than or equal to 8 for cohort 6 only.

(B) Line plots of the total SCFA concentration (log transformed) measured in the stool of healthy volunteers at baseline, after vancomycin administration, or during the recovery period after vancomycin was stopped. The thin lines show the SCFA concentration for individual subjects over time. The thick lines show the median for each cohort over time. In (A and B), the brown dashed line indicates the start of vancomycin administration and the teal dashed line indicates the start of VE303 and/or the start of the recovery from vancomycin.

(C) Random forest regression is used to predict SCFA concentration as a function of microbial abundances. 100 different forests are built by randomly selecting a single sample per patient over 30 random seed initializations. Microbes with a permutated importance p value <0.05 in at least 50% of the 30 × 100 iterations are evaluated with accumulated local effect (ALE; see STAR Methods) analysis. We qualitatively determine positive/negative contribution of each microbe to each measured metabolite using ALE slopes. The annotations reference the *in vitro* SCFA production in Figure S1E. a = *in vitro* acetate >100 µg/log$_{10}$CFU; b = *in vitro* butyrate >30 µg/log$_{10}$CFU.

(Figure 5C). Notably, the associations between VE303 strains and the stool concentration of butyrate and acetate in HVs were largely consistent with the *in vitro* production of SCFAs by the VE303 strains. Seven of the 8 VE303 strains (all but VE303-07 *Longicatena innocuum*) produce acetate *in vitro*, 4 of the 8 strains (VE303-02 *Anaerotruncus colihominis*, VE303-04 *Clostridium_Q symbiosum*, VE303-07 *Longicatena innocuum*, and VE303-08 *Flavonifractor* sp000508885) produce butyrate (Figure S1E). Trace quantities (<1 μg/log$_{10}$CFU) of other SCFAs are also produced by the VE303 strains. The positive associations of VE303-04 and VE303-08 with stool butyrate concentrations further suggest that the functional SCFA phenotype is sustained through LBP dosing, despite the displacement of the endogenous butyrate producers *I. butyriciproducens* and *F. prausnitzii* by VE303 organisms (Figure S4E).

DISCUSSION

Understanding the pretreatment and dosing regimens that maximize LBP colonization is critical to their effective development and clinical application. LBPs based on defined consortia have pharmacological profiles unlike those of existing drug classes such as small molecules or antibody drugs; the live, active ingredients in LBPs are capable of reproducing in the gut and their continued self-renewal leads to their long-term persistence. This non-traditional pharmacologic profile requires distinct approaches to define the colonization of the defined consortium strains and the resident community response to colonization. We used murine models and human FMT results to design an 8-strain bacterial consortium, VE303, which is in clinical development for the prevention of rCDI. In this phase I trial in HVs, we found that VE303 was safe and well tolerated at all doses tested. Importantly, we observed that recipient community depletion with vancomycin was essential for robust and consistent colonization. In addition, we found that following vancomycin-induced depletion of the resident microbiota, administration of multiple doses of VE303 was superior to single VE303 doses, leading to increased and more durable colonization of the consortium members, as evidenced by the AUC values. For this microbiome-based approach, we consider defining the effects of dose and dose frequency on LBP strain colonization to be a surrogate for traditional pharmacokinetic (PK) studies.

Likewise, understanding the effects of an LBP on the resident microbiota and its functions is key to its clinical development. In patients with CDI, vancomycin is routinely administered, resulting in depletion of host beneficial bacteria, lower microbial diversity, and alteration in the gut metabolic state (Contijoch et al., 2019; Manges et al., 2010; Smillie et al., 2018; Staley et al., 2016, 2018; Vincent and Manges, 2015). Individuals with prolonged periods of microbiota disruption following antibiotic treatment are more susceptible to CDI if exposed to *C. difficile* spores (Smits et al., 2016). Thus, we deemed it important to evaluate the effects of VE303 dosing on the resident bacterial community and its functions in both depleted and non-depleted states. For LBPs, we consider this microbiota-focused analysis to be a surrogate for traditional pharmacodynamics (PD) studies. In this HV study, we observed that administration of multiple doses of VE303 following vancomycin was associated with an increase in microbial taxa and metabolites associated with resistance to gut pathogen colo-

nization. This included significant and rapid increases in the abundance of Clostridia, which are known to produce SCFAs and secondary BAs in the gut, and reductions in the abundance of Proteobacteria, which are commonly increased in the gut during disease. We also observed a coincident increase in the concentrations of SCFAs and secondary BAs days after stopping vancomycin in subjects given multiple days of VE303.

Potential mechanisms of action of FMT in patients with rCDI include direct killing of *C. difficile* by FMT species (Dabard et al., 2001; Tvede and Rask-Madsen, 1989), nutrient or ecological competition among FMT species and *C. difficile* (Baktash et al., 2018), and production of gut metabolites that inhibit *C. difficile* growth, toxin production, or promote gut barrier integrity (Buffie et al., 2015; Tam et al., 2020; Thanissery et al., 2017; Theriot et al., 2016). We investigated the ability of VE303 to suppress *C. difficile*, either through direct *in vitro* inhibition or by producing gut metabolites inhibitory to *C. difficile*. The VE303 consortium inhibited the growth of *C. difficile in vitro* (Figure S1A), while strain VE303-06 *Dorea longicatena* was a potent individual inhibitor of *C. difficile* (Figure S1B). Additionally, several VE303 strains were found to produce acetate, butyrate, and propionate *in vitro*, and were positively associated with SCFA concentrations in HV stool. VE303 strain genomes were also found to carry BSH and 7a-, 3a/3b-HSDH genes that encode deconjugation and epimerization steps in the synthesis of secondary BAs from primary BAs (Figure S1D; STAR Methods), and may have particular relevance for the conversion of CDCA to UDCA (Winston and Theriot, 2019). The agreement between the *in silico* predicted BA functions for VE303 and the observed association between VE303 and UDCA concentrations, as well as VE303-associated recovery of endogenous secondary BA-producing taxa suggest that VE303 mediates BA recovery in LBP recipients. These data support a protective role of VE303 against CDI through multiple mechanisms, including direct inhibition, accelerating recovery of a diverse gut microbiota, promoting secondary BA production, and reducing inflammation via SCFA production.

Taken together, we describe the development of a safe, well-tolerated LBP characterized with a pretreatment and dosing regimen that allows for consistent colonization. This phase 1 study provides initial safety data and a clearer understanding of optimal dosing and antibiotic pretreatment requirements for VE303 strain colonization, and the establishment of a bacterial community known to provide resistance to *C. difficile* colonization after antibiotic perturbation.

STAR★METHODS

Detailed methods are provided in the online version of this paper and include the following:

- KEY RESOURCES TABLE
- RESOURCE AVAILABILITY
  - ○ Lead contact
  - ○ Materials availability
  - ○ Data and code availability
- EXPERIMENTAL MODEL AND SUBJECT DETAILS
  - ○ Bacterial strains
  - ○ Experimental animals
  - ○ Human subjects

SUPPLEMENTAL INFORMATION

Supplemental information can be found online at https://doi.org/10.1016/j.chom.2022.03.016.

AUTHOR CONTRIBUTIONS

Conceptualization, M.D., R.M., J.S., Y.-G.K., L.S., R.S., E.J.K., C.P.K., D.B., B.R., J.F., and J.M.N.; software, S.S.M. and N.G.; formal analysis, M.D., R.M., E.C., S.K.B., J.H., A.R.W., and P.H.; investigation, J.S., Y.-G.K., S.R., S.C., C.F., L.C., J.P., and W.S.; resources, S.S.M. and N.G.; data curation, M.D. and R.M.; writing – original draft, M.D., R.M., E.C., S.K.B., N.G., V.B., J.F., and J.M.N.; writing – reviewing & editing, M.D., R.M., E.C., S.K.B., J.S., R.S., B.O., V.B., B.R., J.L.S., J.F., and J.M.N.; visualization, M.D., R.M., E.C., S.K.B., J.H., and J.M.N.; supervision, L.S., B.O., D.B., V.B., B.R., J.F., J.L.S., and J.M.N.; funding acquisition, B.O.

DECLARATION OF INTERESTS

R.M., S.R., E.C., S.C., J.H., C.F., L.C., A.R.W., J.L.S., B.O., and J.M.N. are employees of Vedanta Biosciences and have an equity interest in the company. Vedanta Biosciences holds patents related to this work. M.D., J.S., Y.-G.K., J.P., L.S., R.S., W.S., D.B., and B.R. were employees of Vedanta Biosciences and had an equity interest in the company at the time of their contribution. J.F. is a member of the scientific advisory board of Vedanta Biosciences and has an equity interest in the company. The authors vouch for the accuracy and completeness of the data and data analyses. This content is solely the respon-

sibility of the authors and does not necessarily represent the official views of the Department of Health and Human Services Office of the Assistant Secretary for Preparedness and Response.

INCLUSION AND DIVERSITY

For studies involving human subjects, we worked to ensure gender balance in the recruitment of human subjects. We worked to ensure ethnic or other types of diversity in the recruitment of human subjects. One or more of the authors of this paper self-identifies as an underrepresented ethnic minority in science. One or more of the authors of this paper self-identifies as a member of the LGBTQ+ community. One or more of the authors of this paper self-identifies as living with a disability. The author list of this paper includes contributors from the location where the research was conducted who participated in the data collection, design, analysis, and/or interpretation of the work.

REFERENCES

Administration US Food and Drug (2011). Early Clinical Trials with Live Biotherapeutic Products: Chemistry, Manufacturing, and Control Information (FDA).

Aggarwala, V., Mogno, I., Li, Z., Yang, C., Britton, G.J., Chen-Liaw, A., Mitcham, J., Bongers, G., Gevers, D., Clemente, J.C., et al. (2021). Precise quantification of bacterial strains after fecal microbiota transplantation delineates long-term engraftment and explains outcomes. Nat. Microbiol. *6*, 1309–1318.

Aitoro, R., Paparo, L., Amoroso, A., Di Costanzo, M., Cosenza, L., Granata, V., Di Scala, C., Nocerino, R., Trinchese, G., Montella, M., et al. (2017). Gut microbiota as a target for preventive and therapeutic intervention against food allergy. Nutrients *9*, 672.

Allain, T., Chaouch, S., Thomas, M., Vallée, I., Buret, A.G., Langella, P., Grellier, P., Polack, B., Bermúdez-Humarán, L.G., and Florent, I. (2017). Bile-salt-hydrolases from the probiotic strain *Lactobacillus johnsonii* La1 mediate antigiardial activity *in vitro* and *in vivo*. Front. Microbiol. *8*, 2707.

Allegretti, J.R., Kassam, Z., Mullish, B.H., Chiang, A., Carrellas, M., Hurtado, J., Marchesi, J.R., McDonald, J.A.K., Pechlivanis, A., Barker, G.F., et al. (2020). Effects of fecal microbiota transplantation with oral capsules in obese patients. Clin. Gastroenterol. Hepatol. *18*, 855–863.e2.

Altmann, A., Toloşi, L., Sander, O., and Lengauer, T. (2010). Permutation importance: a corrected feature importance measure. Bioinformatics *26*, 1340–1347.

Altschul, S.F., Gish, W., Miller, W., Myers, E.W., and Lipman, D.J. (1990). Basic local alignment search tool. J. Mol. Biol. *215*, 403–410.

Antharam, V.C., Li, E.C., Ishmael, A., Sharma, A., Mai, V., Rand, K.H., and Wang, G.P. (2013). Intestinal dysbiosis and depletion of butyrogenic bacteria in *Clostridium difficile* infection and nosocomial diarrhea. J. Clin. Microbiol. *51*, 2884–2892.

Apley, D.W., and Zhu, J. (2020). Visualizing the effects of predictor variables in Black box supervised learning models. J. R. Stat. Soc. B *82*, 1059–1086.

Atarashi, K., Tanoue, T., Ando, M., Kamada, N., Nagano, Y., Narushima, S., Suda, W., Imaoka, A., Setoyama, H., Nagamori, T., et al. (2015). Th17 cell induction by adhesion of microbes to intestinal epithelial cells. Cell *163*, 367–380.

Atarashi, K., Tanoue, T., Oshima, K., Suda, W., Nagano, Y., Nishikawa, H., Fukuda, S., Saito, T., Narushima, S., Hase, K., et al. (2013). Treg induction by a rationally selected mixture of *Clostridia* strains from the human microbiota. Nature *500*, 232–236.

Bakken, J.S., Borody, T., Brandt, L.J., Brill, J.V., Demarco, D.C., Franzos, M.A., Kelly, C., Khoruts, A., Louie, T., Martinelli, L.P., et al. (2011). Treating *Clostridium difficile* infection with fecal microbiota transplantation. Clin. Gastroenterol. Hepatol. *9*, 1044–1049.

Baktash, A., Terveer, E.M., Zwittink, R.D., Hornung, B.V.H., Corver, J., Kuijper, E.J., and Smits, W.K. (2018). Mechanistic insights in the success of fecal microbiota transplants for the treatment of *Clostridium difficile* infections. Front. Microbiol. *9*, 1242.

Belkaid, Y., and Hand, T.W. (2014). Role of the microbiota in immunity and inflammation. Cell *157*, 121–141.

Bishehsari, F., Engen, P.A., Preite, N.Z., Tuncil, Y.E., Naqib, A., Shaikh, M., Rossi, M., Wilber, S., Green, S.J., Hamaker, B.R., et al. (2018). Dietary fiber treatment corrects the composition of gut microbiota, promotes SCFA production, and suppresses colon carcinogenesis. Genes (Basel) *9*, 102.

Blaser, M.J. (2019). Fecal microbiota transplantation for dysbiosis—predictable risks. N. Engl. J. Med. *381*, 2064–2066.

Blin, K., Wolf, T., Chevrette, M.G., Lu, X., Schwalen, C.J., Kautsar, S.A., Suarez Duran, H.G., de Los Santos, E.L.C., Kim, H.U., Nave, M., et al. (2017). antiSMASH 4.0—improvements in chemistry prediction and gene cluster boundary identification. Nucleic Acids Res. *45*, W36–W41.

Blount, K., Jones, C., Deych, E., and Shannon, B. (2018). Developing Microbiome Rehabilitation Biomarkers for Clostridium Difficile Infections: Continued Evaluation of a Prototype Microbiome Health Index™ (MHI™) (Rebiotix Inc.).

Britton, G.J., Chen-Liaw, A., Cossarini, F., Livanos, A.E., Spindler, M.P., Plitt, T., Eggers, J., Mogno, I., Gonzalez-Reiche, A.S., Siu, S., et al. (2021). Limited intestinal inflammation despite diarrhea, fecal viral RNA and SARS-CoV-2-specific IgA in patients with acute COVID-19. Sci. Rep. *11*, 13308.

Buffie, C.G., Bucci, V., Stein, R.R., McKenney, P.T., Ling, L., Gobourne, A., Liu, H., Kinnebrew, M., Viale, A., et al. (2015). Precision microbiome reconstitution restores bile acid mediated resistance to *Clostridium difficile*. Nature *517*, 205–208.

Bushnell, B. (2014). BBTools software package. URL http://sourceforge.net/projects/bbmap *578*, 579.

Cait, A., Hughes, M.R., Antignano, F., Cait, J., Dimitriu, P.A., Maas, K.R., Reynolds, L.A., Hacker, L., Mohr, J., Finlay, B.B., et al. (2018). Microbiome-driven allergic lung inflammation is ameliorated by short-chain fatty acids. Mucosal Immunol. *11*, 785–795.

Chaumeil, P.-A., Mussig, A.J., Hugenholtz, P., and Parks, D.H. (2019). GTDB-Tk: a toolkit to classify genomes with the Genome Taxonomy Database. Bioinformatics *36*, 1925–1927.

Chen, E.Z., and Li, H. (2016). A two-part mixed-effects model for analyzing longitudinal microbiome compositional data. Bioinformatics *32*, 2611–2617.

Chen, M.L., Takeda, K., and Sundrud, M.S. (2019). Emerging roles of bile acids in mucosal immunity and inflammation. Mucosal Immunol. *12*, 851–861.

Chen, S., Zhou, Y., Chen, Y., and Gu, J. (2018). fastp: an ultra-fast all-in-one FASTQ preprocessor. Bioinformatics *34*, i884–i890.

Cock, P.J.A., Antao, T., Chang, J.T., Chapman, B.A., Cox, C.J., Dalke, A., Friedberg, I., Hamelryck, T., Kauff, F., Wilczynski, B., and de Hoon, M.J. (2009). Biopython: freely available Python tools for computational molecular biology and bioinformatics. Bioinformatics *25*, 1422–1423.

Cock, P.J.A., Chilton, J.M., Grüning, B., Johnson, J.E., and Soranzo, N. (2015). NCBI Blast+ integrated into Galaxy. GigaScience *4*, 39.

Collins, M.D., Lawson, P.A., Willems, A., Cordoba, J.J., Fernandez-Garayzabal, J., Garcia, P., Cai, J., Hippe, H., and Farrow, J.A. (1994). The phylogeny of the genus Clostridium: proposal of five new genera and eleven new species combinations. Int. J. Syst. Bacteriol. *44*, 812–826.

Contijoch, E.J., Britton, G.J., Yang, C., Mogno, I., Li, Z., Ng, R., Llewellyn, S.R., Hira, S., Johnson, C., Rabinowitz, K.M., et al. (2019). Gut microbiota density influences host physiology and is shaped by host and microbial factors. Elife *8*, e40553.

Costello, S.P., Conlon, M.A., Vuaran, M.S., Roberts-Thomson, I.C., and Andrews, J.M. (2015). Faecal microbiota transplant for recurrent *Clostridium difficile* infection using long-term frozen stool is effective: clinical efficacy and bacterial viability data. Aliment. Pharmacol. Ther. *42*, 1011–1018.

Costello, S.P., Hughes, P.A., Waters, O., Bryant, R.V., Vincent, A.D., Blatchford, P., Katsikeros, R., Makanyanga, J., Campaniello, M.A., Mavrangelos, C., et al. (2019). Effect of fecal microbiota transplantation on

8-week remission in patients with ulcerative colitis: a randomized clinical trial. JAMA *321*, 156–164.

Dabard, J., Bridonneau, C., Phillipe, C., Anglade, P., Molle, D., Nardi, M., Ladiré, M., Girardin, H., Marcille, F., Gomez, A., and Fons, M. (2001). Ruminococcin A, a new lantibiotic produced by a *Ruminococcus gnavus* strain isolated from human feces. Appl. Environ. Microbiol. *67*, 4111–4118.

DeFilipp, Z., Bloom, P.P., Torres Soto, M., Mansour, M.K., Sater, M.R.A., Huntley, M.H., Turbett, S., Chung, R.T., Chen, Y.-B., and Hohmann, E.L. (2019). Drug-resistant *E. coli* bacteremia transmitted by fecal microbiota transplant. N. Engl. J. Med. *381*, 2043–2050.

Devlin, A.S., and Fischbach, M.A. (2015). A biosynthetic pathway for a prominent class of microbiota-derived bile acids. Nat. Chem. Biol. *11*, 685–690.

Dianawati, D., Mishra, V., and Shah, N.P. (2016). Survival of microencapsulated probiotic bacteria after processing and during storage: a review. Crit. Rev. Food Sci. Nutr. *56*, 1685–1716.

Doden, H., Sallam, L.A., Devendran, S., Ly, L., Doden, G., Daniel, S.L., Alves, J.M.P., and Ridlon, J.M. (2018). Metabolism of oxo-bile acids and characterization of recombinant 12α-Hydroxysteroid dehydrogenases from bile acid 7α-Dehydroxylating human gut bacteria. Appl. Environ. Microbiol. *84*.

Donohoe, D.R., Holley, D., Collins, L.B., Montgomery, S.A., Whitmore, A.C., Hillhouse, A., Curry, K.P., Renner, S.W., Greenwalt, A., Ryan, E.P., et al. (2014). A gnotobiotic mouse model demonstrates that dietary fiber protects against colorectal tumorigenesis in a microbiota- and butyrate-dependent manner. Cancer Discov. *4*, 1387–1397.

Drewes, J.L., Corona, A., Sanchez, U., Fan, Y., Hourigan, S.K., Weidner, M., Sidhu, S.D., Simner, P.J., Wang, H., Timp, W., et al. (2019). Transmission and clearance of potential procarcinogenic bacteria during fecal microbiota transplantation for recurrent *Clostridioides difficile*. JCI Insight *4*, e130848.

Fachi, J.L., Felipe, J.S., Pral, L.P., da Silva, B.K., Corrêa, R.O., de Andrade, M.C.P., da Fonseca, D.M., Basso, P.J., Câmara, N.O.S., de Sales E Souza, É.L., et al. (2019). Butyrate protects mice from *Clostridium difficile*-induced colitis through an HIF-1-dependent mechanism. Cell Rep. *27*, 750–761.e7.

Faith, J.J., McNulty, N.P., Rey, F.E., and Gordon, J.I. (2011). Predicting a human gut microbiota's response to diet in gnotobiotic mice. Science *333*, 101–104.

Ferretti, P., Pasolli, E., Tett, A., Asnicar, F., Gorfer, V., Fedi, S., Armanini, F., Truong, D.T., Manara, S., Zolfo, M., et al. (2018). Mother-to-infant microbial transmission from different body sites shapes the developing infant gut microbiome. Cell Host Microbe *24*, 133–145.e5.

Foley, M.H., O'Flaherty, S., Barrangou, R., and Theriot, C.M. (2019). Bile salt hydrolases: gatekeepers of bile acid metabolism and host-microbiome crosstalk in the gastrointestinal tract. PLoS Pathog. *15*, e1007581.

Food and Drug Administration (2013). Good review practice: clinical review of investigational new drug applications, https://www.fda.gov/media/87621/download.

Fu, L., Niu, B., Zhu, Z., Wu, S., and Li, W. (2012). CD-HIT: accelerated for clustering the next-generation sequencing data. Bioinformatics *28*, 3150–3152.

Fuentes, S., Rossen, N.G., van der Spek, M.J., Hartman, J.H., Huuskonen, L., Korpela, K., Salojärvi, J., Aalvink, S., de Vos, W.M., D'Haens, G.R., et al. (2017). Microbial shifts and signatures of long-term remission in ulcerative colitis after faecal microbiota transplantation. ISME J. *11*, 1877–1889.

Furusawa, Y., Obata, Y., Fukuda, S., Endo, T.A., Nakato, G., Takahashi, D., Nakanishi, Y., Uetake, C., Kato, K., Kato, T., et al. (2013). Commensal microbe-derived butyrate induces the differentiation of colonic regulatory T cells. Nature *504*, 446–450.

Geva-Zatorsky, N., Sefik, E., Kua, L., Pasman, L., Tan, T.G., Ortiz-Lopez, A., Yanortsang, T.B., Yang, L., Jupp, R., Mathis, D., et al. (2017). Mining the human gut microbiota for immunomodulatory organisms. Cell *168*, 928–943.e11.

Hamilton, M.J., Weingarden, A.R., Unno, T., Khoruts, A., and Sadowsky, M.J. (2013). High-throughput DNA sequence analysis reveals stable engraftment of gut microbiota following transplantation of previously frozen fecal bacteria. Gut Microbes *4*, 125–135.

Haran, J.P., Bhattarai, S.K., Foley, S.E., Dutta, P., Ward, D.V., Bucci, V., and McCormick, B.A. (2019). Alzheimer's disease microbiome is associated with

dysregulation of the anti-inflammatory *P*-glycoprotein pathway. mBio *10*, e00632–e00619.

Heinken, A., Ravcheev, D.A., Baldini, F., Heirendt, L., Fleming, R.M.T., and Thiele, I. (2019). Systematic assessment of secondary bile acid metabolism in gut microbes reveals distinct metabolic capabilities in inflammatory bowel disease. Microbiome *7*, 75.

Henn, M.R., O'Brien, E.J., Diao, L., Feagan, B.G., Sandborn, W.J., Huttenhower, C., Wortman, J.R., McGovern, B.H., Wang-Weigand, S., Lichter, D.I., et al. (2021). A phase 1b safety study of SER-287, a spore-based microbiome therapeutic, for active mild to moderate ulcerative colitis. Gastroenterology *160*, 115–127.e30.

Hensgens, M.P.M., Goorhuis, A., Dekkers, O.M., and Kuijper, E.J. (2012). Time interval of increased risk for *Clostridium difficile* infection after exposure to antibiotics. J. Antimicrob. Chemother. *67*, 742–748.

Isabella, V.M., Ha, B.N., Castillo, M.J., Lubkowicz, D.J., Rowe, S.E., Millet, Y.A., Anderson, C.L., Li, N., Fisher, A.B., West, K.A., et al. (2018). Development of a synthetic live bacterial therapeutic for the human metabolic disease phenylketonuria. Nat. Biotechnol. *36*, 857–864.

G. Jagschies, E. Lindskog, K. Lacki, and P.M. Galliher, eds. (2018). Biopharmaceutical Processing: Development, Design, and Implementation of Manufacturing Processes (Elsevier).

Kang, J.D., Myers, C.J., Harris, S.C., Kakiyama, G., Lee, I.-K., Yun, B.-S., Matsuzaki, K., Furukawa, M., Min, H.-K., Bajaj, J.S., et al. (2019). Bile acid 7α-Dehydroxylating gut bacteria secrete antibiotics that inhibit *Clostridium difficile*: role of secondary bile acids. Cell Chem. Biol. *26*, 27–34.e4.

Kao, D., Roach, B., Silva, M., Beck, P., Rioux, K., Kaplan, G.G., Chang, H.J., Coward, S., Goodman, K.J., Xu, H., et al. (2017). Effect of Oral capsule- *vs* colonoscopy-delivered fecal microbiota transplantation on recurrent *Clostridium difficile* infection: a randomized clinical trial. JAMA *318*, 1985–1993.

Kao, D., Wong, K., Franz, R., Cochrane, K., Sherriff, K., Chui, L., Lloyd, C., Roach, B., Bai, A.D., Petrof, E.O., and Allen-Vercoe, E. (2021). The effect of a microbial ecosystem therapeutic (MET-2) on recurrent Clostridioides *difficile* infection: a phase 1, open-label, single-group trial. Lancet Gastroenterol. Hepatol. *6*, 282–291.

Kelly, C.R., Ihunnah, C., Fischer, M., Khoruts, A., Surawicz, C., Afzali, A., Aroniadis, O., Barto, A., Borody, T., Giovanelli, A., et al. (2014). Fecal microbiota transplant for treatment of *Clostridium difficile* infection in immunocompromised patients. Am. J. Gastroenterol. *109*, 1065–1071.

Kim, M., Friesen, L., Park, J., Kim, H.M., and Kim, C.H. (2018). Microbial metabolites, short-chain fatty acids, restrain tissue bacterial load, chronic inflammation, and associated cancer in the colon of mice. Eur. J. Immunol. *48*, 1235–1247.

Kolmogorov, M., Yuan, J., Lin, Y., and Pevzner, P.A. (2019). Assembly of long, error-prone reads using repeat graphs. Nat. Biotechnol. *37*, 540–546.

Konturek, P.C., Koziel, J., Dieterich, W., Haziri, D., Wirtz, S., Glowczyk, I., Konturek, K., Neurath, M.F., and Zopf, Y. (2016). Successful therapy of *Clostridium difficile* infection with fecal microbiota transplantation. J. Physiol. Pharmacol. *67*, 859–866.

Korpela, K., Costea, P., Coelho, L.P., Kandels-Lewis, S., Willemsen, G., Boomsma, D.I., Segata, N., and Bork, P. (2018). Selective maternal seeding and environment shape the human gut microbiome. Genome Res. *28*, 561–568.

Langmead, B., and Salzberg, S.L. (2012). Fast gapped-read alignment with Bowtie 2. Nat. Methods *9*, 357–359.

Levine, D.P. (2006). Vancomycin: a history. Clin. Infect. Dis. *42* (suppl. 1), S5–S12.

Li, H. (2013). Aligning sequence reads, clone sequences and assembly contigs with BWA-MEM. Preprint at arXiv. arXiv:1303.3997.

Livanos, A.E., Jha, D., Cossarini, F., Gonzalez-Reiche, A.S., Tokuyama, M., Aydillo, T., Parigi, T.L., Ladinsky, M.S., Ramos, I., Dunleavy, K., et al. (2021). Intestinal host response to SARS-CoV-2 infection and COVID-19 outcomes in patients With gastrointestinal symptoms. Gastroenterology *160*, 2435–2450, e34.

Llewellyn, S.R., Britton, G.J., Contijoch, E.J., Vennaro, O.H., Mortha, A., Colombel, J.-F., Grinspan, A., Clemente, J.C., Merad, M., and Faith, J.J.

(2018). Interactions between diet and the intestinal microbiota alter intestinal permeability and colitis severity in mice. Gastroenterology *154*, 1037–1046.e2.

Luethy, P.M., Huynh, S., Ribardo, D.A., Winter, S.E., Parker, C.T., and Hendrixson, D.R. (2017). Microbiota-derived short-chain fatty acids modulate expression of *Campylobacter jejuni* determinants required for commensalism and virulence. mBio *8*, e00407–e00417.

Manfredo Vieira, S., Hiltensperger, M., Kumar, V., Zegarra-Ruiz, D., Dehner, C., Khan, N., Costa, F.R.C., Tiniakou, E., Greiling, T., Ruff, W., et al. (2018). Translocation of a gut pathobiont drives autoimmunity in mice and humans. Science *359*, 1156–1161.

Manges, A.R., Labbe, A., Loo, V.G., Atherton, J.K., Behr, M.A., Masson, L., Tellis, P.A., and Brousseau, R. (2010). Comparative metagenomic study of alterations to the intestinal microbiota and risk of nosocomial Clostridum *difficile*-associated disease. J. Infect. Dis. *202*, 1877–1884.

McDonald, L.C., Gerding, D.N., Johnson, S., Bakken, J.S., Carroll, K.C., Coffin, S.E., Dubberke, E.R., Garey, K.W., Gould, C.V., Kelly, C., et al. (2018). Clinical practice guidelines for *Clostridium difficile* infection in adults and children: 2017 update by the Infectious Diseases Society of America (IDSA) and Society for Healthcare Epidemiology of America (SHEA). Clin. Infect. Dis. *66*, e1–e48.

McGovern, B.H., Ford, C.B., Henn, M.R., Pardi, D.S., Khanna, S., Hohmann, E.L., O'Brien, E.J., Desjardins, C.A., Bernardo, P., Wortman, J.R., et al. (2021). SER-109, an investigational microbiome drug to reduce recurrence after *Clostridioides difficile* infection: lessons learned From a Phase 2 trial. Clin. Infect. Dis. *72*, 2132–2140.

Minot, S.S., Krumm, N., and Greenfield, N.B. (2015). One Codex: a sensitive and accurate data platform for genomic microbial identification. Preprint at bioRxiv. https://doi.org/10.1101/027607.

Moayyedi, P., Surette, M.G., Kim, P.T., Libertucci, J., Wolfe, M., Onischi, C., Armstrong, D., Marshall, J.K., Kassam, Z., Reinisch, W., et al. (2015). Fecal microbiota transplantation induces remission in patients with active ulcerative colitis in a randomized controlled trial. Gastroenterology *149*, 102–109.e6.

Nayfach, S., and Pollard, K.S. (2016). Toward accurate and quantitative comparative metagenomics. Cell *166*, 1103–1116.

Nooij, S., Ducarmon, Q.R., Laros, J.F.J., Zwittink, R.D., Norman, J.M., Smits, W.K., Verspaget, H.W., Keller, J.J., Terveer, E.M., and Kuijper, E.J. (2021). Faecal microbiota transplantation influences procarcinogenic *Escherichia coli* in recipient recurrent *Clostridioides difficile* patients. Gastroenterology *161*, 1218–1228.e5.

Olm, M.R., Crits-Christoph, A., Bouma-Gregson, K., Firek, B.A., Morowitz, M.J., and Banfield, J.F. (2021). inStrain profiles population microdiversity from metagenomic data and sensitively detects shared microbial strains. Nat. Biotechnol. *39*, 727–736.

Palleja, A., Mikkelsen, K.H., Forslund, S.K., Kashani, A., Allin, K.H., Nielsen, T., Hansen, T.H., Liang, S., Feng, Q., Zhang, C., et al. (2018). Recovery of gut microbiota of healthy adults following antibiotic exposure. Nat. Microbiol. *3*, 1255–1265.

Palmieri, L.-J., Rainteau, D., Sokol, H., Beaugerie, L., Dior, M., Coffin, B., Humbert, L., Eguether, T., Bado, A., Hoys, S., et al. (2018). Inhibitory effect of ursodeoxycholic acid on *Clostridium difficile* germination is insufficient to prevent colitis: a study in hamsters and humans. Front. Microbiol. *9*, 2849.

Petrof, E.O., Gloor, G.B., Vanner, S.J., Weese, S.J., Carter, D., Daigneault, M.C., Brown, E.M., Schroeter, K., and Allen-Vercoe, E. (2013). Stool substitute transplant therapy for the eradication of *Clostridium difficile* infection: "RePOOPulating" the gut. Microbiome *1*, 3.

R Core Team (2021). *R*: A language and environment for statistical computing (R Foundation for Statistical Computing). https://www.R-project.org/.

Ramai, D., Zakhia, K., Fields, P.J., Ofosu, A., Patel, G., Shahnazarian, V., Lai, J.K., Dhaliwal, A., Reddy, M., and Chang, S. (2021). Fecal microbiota transplantation (FMT) with colonoscopy is superior to enema and nasogastric tube while comparable to capsule for the treatment of recurrent *Clostridioides difficile* infection: a systematic review and meta-analysis. Dig. Dis. Sci. *66*, 369–380.

Reyes, A., Wu, M., McNulty, N.P., Rohwer, F.L., and Gordon, J.I. (2013). Gnotobiotic mouse model of phage-bacterial host dynamics in the human gut. Proc. Natl. Acad. Sci. USA *110*, 20236–20241.

Ridlon, J.M., Harris, S.C., Bhowmik, S., Kang, D.J., and Hylemon, P.B. (2016). Consequences of bile salt biotransformations by intestinal bacteria. Gut Microbes *7*, 22–39.

Ridlon, J.M., Kang, D.-J., and Hylemon, P.B. (2010). Isolation and characterization of a bile acid inducible 7alpha-dehydroxylating operon in *Clostridium hylemonae* TN271. Anaerobe *16*, 137–146.

Rubin, T.A., Gessert, C.E., Aas, J., and Bakken, J.S. (2013). Fecal microbiome transplantation for recurrent *Clostridium difficile* infection: report on a case series. Anaerobe *19*, 22–26.

Seekatz, A.M., Rao, K., Santhosh, K., and Young, V.B. (2016). Dynamics of the fecal microbiome in patients with recurrent and nonrecurrent *Clostridium difficile* infection. Genome Med. *8*, 47.

Seekatz, A.M., Theriot, C.M., Rao, K., Chang, Y.-M., Freeman, A.E., Kao, J.Y., and Young, V.B. (2018). Restoration of short chain fatty acid and bile acid metabolism following fecal microbiota transplantation in patients with recurrent *Clostridium difficile* infection. Anaerobe *53*, 64–73.

Seemann, T. (2014). Prokka: rapid prokaryotic genome annotation. Bioinformatics *30*, 2068–2069.

Smillie, C.S., Sauk, J., Gevers, D., Friedman, J., Sung, J., Youngster, I., Hohmann, E.L., Staley, C., Khoruts, A., Sadowsky, M.J., et al. (2018). Strain tracking reveals the determinants of bacterial engraftment in the human gut following fecal microbiota transplantation. Cell Host Microbe *23*, 229–240.e5.

Smits, W.K., Lyras, D., Lacy, D.B., Wilcox, M.H., and Kuijper, E.J. (2016). *Clostridium difficile* infection. Nat. Rev. Dis. Primers *2*, 16020.

Sorg, J.A., and Sonenshein, A.L. (2008). Bile salts and glycine as cogerminants for *Clostridium difficile* spores. J. Bacteriol. *190*, 2505–2512.

Sprouffske, K., and Wagner, A. (2016). Growthcurver: an R package for obtaining interpretable metrics from microbial growth curves. BMC Bioinformatics *17*, 172.

Staley, C., Kaiser, T., Vaughn, B.P., Graiziger, C.T., Hamilton, M.J., Rehman, T.U., Song, K., Khoruts, A., and Sadowsky, M.J. (2018). Predicting recurrence of *Clostridium difficile* infection following encapsulated fecal microbiota transplantation. Microbiome *6*, 166.

Staley, C., Kelly, C.R., Brandt, L.J., Khoruts, A., and Sadowsky, M.J. (2016). Complete microbiota engraftment is not essential for recovery from recurrent *Clostridium difficile* Infection following Fecal microbiota Transplantation. mBio *7*, e01965–e01916.

Sze, M.A., and Schloss, P.D. (2016). Looking for a signal in the noise: revisiting obesity and the microbiome. mBio *7*, e01018–e01016.

Tam, J., Icho, S., Utama, E., Orrell, K.E., Gómez-Biagi, R.F., Theriot, C.M., Kroh, H.K., Rutherford, S.A., Lacy, D.B., and Melnyk, R.A. (2020). Intestinal bile acids directly modulate the structure and function of *C. difficile* TcdB toxin. Proc. Natl. Acad. Sci. USA *117*, 6792–6800.

Tan, J., McKenzie, C., Vuillermin, P.J., Goverse, G., Vinuesa, C.G., Mebius, R.E., Macia, L., and Mackay, C.R. (2016). Dietary fiber and bacterial SCFA enhance oral tolerance and protect against food allergy through diverse cellular pathways. Cell Rep. *15*, 2809–2824.

Tanoue, T., Morita, S., Plichta, D.R., Skelly, A.N., Suda, W., Sugiura, Y., Narushima, S., Vlamakis, H., Motoo, I., Sugita, K., et al. (2019). A defined commensal consortium elicits CD8 T cells and anti-cancer immunity. Nature *565*, 600–605.

Thanissery, R., Winston, J.A., and Theriot, C.M. (2017). Inhibition of spore germination, growth, and toxin activity of clinically relevant *C. difficile* strains by gut microbiota derived secondary bile acids. Anaerobe *45*, 86–100.

Theriot, C.M., Bowman, A.A., and Young, V.B. (2016). Antibiotic-induced alterations of the gut microbiota alter secondary bile acid production and allow for *Clostridium difficile* Spore germination and outgrowth in the large intestine. mSphere *1*, e00045–e00015.

Theriot, C.M., Koumpouras, C.C., Carlson, P.E., Bergin, I.I., Aronoff, D.M., and Young, V.B. (2011). Cefoperazone-treated mice as an experimental platform to assess differential virulence of *Clostridium difficile* strains. Gut Microbes *2*, 326–334.

Theriot, C.M., Koenigsknecht, M.J., Carlson, P.E., Hatton, G.E., Nelson, A.M., Li, B., Huffnagle, G.B., Z Li, J., and Young, V.B. (2014). Antibiotic-induced shifts in the mouse gut microbiome and metabolome increase susceptibility to *Clostridium difficile* infection. Nat. Commun. *5*, 3114.

Tvede, M., and Rask-Madsen, J. (1989). Bacteriotherapy for chronic relapsing *Clostridium difficile* diarrhoea in six patients. Lancet *1*, 1156–1160.

U.S. Food and Drug Administration (2020). Safety Alert Regarding Use of Fecal Microbiota for Transplantation and Risk of Serious Adverse Events Likely Due to Transmission of Pathogenic Organisms (FDA).

van Nood, E., Vrieze, A., Nieuwdorp, M., Fuentes, S., Zoetendal, E.G., de Vos, W.M., Visser, C.E., Kuijper, E.J., Bartelsman, J.F.W.M., Tijssen, J.G.P., et al. (2013). Duodenal infusion of donor feces for recurrent *Clostridium difficile*. N. Engl. J. Med. *368*, 407–415.

Vaser, R., and Šikić, M. (2021). Time- and memory-efficient genome assembly with Raven. Nat. Comput. Sci. *1*, 332–336.

Vaser, R., Sović, I., Nagarajan, N., and Šikić, M. (2017). Fast and accurate *de novo* genome assembly from long uncorrected reads. Genome Res. *27*, 737–746.

Villano, S.A., Seiberling, M., Tatarowicz, W., Monnot-Chase, E., and Gerding, D.N. (2012). Evaluation of an oral suspension of VP20621, spores of nontoxigenic *Clostridium difficile strain* M3, in healthy subjects. Antimicrob. Agents Chemother. *56*, 5224–5229.

Vincent, C., and Manges, A.R. (2015). Antimicrobial use, human gut microbiota and *Clostridium difficile* colonization and infection. Antibiotics (Basel) *4*, 230–253.

Walker, B.J., Abeel, T., Shea, T., Priest, M., Abouelliel, A., Sakthikumar, S., Cuomo, C.A., Zeng, Q., Wortman, J., Young, S.K., and Earl, A.M. (2014). Pilon: an integrated tool for comprehensive microbial variant detection and genome assembly improvement. PLoS One *9*, e112963.

Wang, W., Xu, Y., Gao, R., Lu, R., Han, K., Wu, G., and Tan, W. (2020). Detection of SARS-CoV-2 in different types of clinical specimens. JAMA *323*, 1843–1844.

Weingarden, A.R., Chen, C., Zhang, N., Graiziger, C.T., Dosa, P.I., Steer, C.J., Shaughnessy, M.K., Johnson, J.R., Sadowsky, M.J., and Khoruts, A. (2016). Ursodeoxycholic acid inhibits *Clostridium difficile* Spore germination and vegetative growth, and prevents the recurrence of ileal Pouchitis associated with the infection. J. Clin. Gastroenterol. *50*, 624–630.

Wick, R.R., and Holt, K.E. (2022). Polypolish: short-read polishing of long-read bacterial genome assemblies. PLoS Comp. Biol. *18*, e1009802.

Wick, R.R., and Menzel, P. (2019). Filtlong: quality filtering tool for long reads, https://github.com/rrwick/Filtlong.

Winston, J.A., and Theriot, C.M. (2019). Diversification of host bile acids by members of the gut microbiota. Gut Microbes *11*, 158–171.

Xu, D., Chen, V.L., Steiner, C.A., Berinstein, J.A., Eswaran, S., Waljee, A.K., Higgins, P.D.R., and Owyang, C. (2019). Efficacy of fecal microbiota transplantation in irritable bowel syndrome: a systematic review and meta-analysis. Am. J. Gastroenterol. *114*, 1043–1050.

Youngster, I., Mahabamunuge, J., Systrom, H.K., Sauk, J., Khalili, H., Levin, J., Kaplan, J.L., and Hohmann, E.L. (2016). Oral, frozen fecal microbiota transplant (FMT) capsules for recurrent *Clostridium difficile* infection. BMC Med. *14*, 134.

Zhao, L., Zhang, F., Ding, X., Wu, G., Lam, Y.Y., Wang, X., Fu, H., Xue, X., Lu, C., Ma, J., et al. (2018). Gut bacteria selectively promoted by dietary fibers alleviate type 2 diabetes. Science *359*, 1151–1156.

Zou, J., Chassaing, B., Singh, V., Pellizzon, M., Ricci, M., Fythe, M.D., Kumar, M.V., and Gewirtz, A.T. (2018). Fiber-mediated nourishment of gut microbiota protects against diet-induced obesity by restoring IL-22-mediated colonic health. Cell Host Microbe *23*, 41–53.e4.

STAR★METHODS

KEY RESOURCES TABLE

REAGENT or RESOURCE	SOURCE	IDENTIFIER
Bacterial and virus strains		
Clostridioides difficile VPI 10463	ATCC	ATCC 43255
Clostridium bifermentans	This paper	N/A
Lactobacillus ruminis	This paper	N/A
VE303-01	This paper	N/A
VE303-02	This paper	N/A
VE303-03	This paper	N/A
VE303-04	This paper	N/A
VE303-05	This paper	N/A
VE303-06	This paper	N/A
VE303-07	This paper	N/A
VE303-08	This paper	N/A
Critical commercial assays		
MasterPure™ Complete DNA and RNA Purification Kit	Epicentre	Cat No. MC85200
TruSeq DNA PCR-Free Library Prep	Illumina	Cat no. 20015963
Kapa Biosystems Illumina Library Quantification Real Time PCR assay	Roche	Cat No. 07960727001
SMRTbell Template Preparation	Pacific Biosciences	Cat No. 100-259-100
PowerMag® Microbiome RNA/DNA Isolation Kit	MO BIO Laboratories	Cat No. 27500-4-EP
Deposited data		
VE303 marker panel sequences	This paper	Table S4
VE303 strain genomes	This paper	NCBI BioProject: PRJNA755324
Metagenomic sequences	This paper	NCBI BioProject: PRJNA755324
Data analyses code	This paper	https://gitlab.com/vedantabio-public/ve303-phase-1
Experimental models: Organisms/strains		
Mouse: C57BL/6: Female 6-8 week old	The Jackson Laboratory	N/A
Software and algorithms		
Gen5 software	BioTek Instruments	https://www.biotek.com/products/software-robotics/
antiSMASH 4.0	Blin et al., 2017	https://antismash.secondarymetabolites.org/#!/start
BLASTx	Altschul et al., 1990	https://blast.ncbi.nlm.nih.gov/Blast.cgi
PROKKA	Seemann, 2014	https://github.com/tseemann/prokka
BLAST+ Galaxy integrated toolset	Cock et al., 2015	https://github.com/peterjc/galaxy_blast
BBTools	Bushnell B.	sourceforge.net/projects/bbmap/
One Codex platform	N/A	https://www.onecodex.com/
ZIBR (Zero-Inflated Beta Random) Effect model	Chen and Li, 2016	https://github.com/chvlyl/ZIBR
Prism GraphPad software v8.0	GraphPad Software	https://www.graphpad.com/scientific-software/prism/

(Continued on next page)

Continued

REAGENT or RESOURCE	SOURCE	IDENTIFIER
VE303 strain detection algorithm	This paper	N/A
BioPython	Cock et al., 2009	https://biopython.org/
R software v3.5.3	R Core Team, 2021	https://www.r-project.org/
Other		
GTDB-Tk (database version 89)	Chaumeil et al., 2019	https://gtdb.ecogenomic.org/downloads

RESOURCE AVAILABILITY

Lead contact
Further information and requests for resources and reagents should be directed to and will be fulfilled by the lead contact, Jason M. Norman (jnorman@vedantabio.com).

Materials availability
The authors agree to make all unique biological materials and generated resources including isolated strains available to the research community upon request and after establishing a Materials Transfer Agreement with Vedanta Biosciences, Inc. Correspondence should be addressed to legal@vedantabio.com and the lead contact, Jason M. Norman.

Data and code availability
Whole-genome sequence and metagenomic sequence data have been deposited at the National Center for Biotechnology Information (NCBI) and are publicly available as of the date of publication. Accession numbers are listed in the key resources table. All data associated with this study are presented in the paper or the supplemental information. All original code has been deposited on GitLab (https://gitlab.com/vedantabio-public/ve303-phase-1) and is publicly available as of the date of publication. Any additional information required to reanalyze the data reported in this paper is available from the lead contact upon request.

EXPERIMENTAL MODEL AND SUBJECT DETAILS

Bacterial strains
Each of the bacterial strains in VE303 was isolated from a single colony grown on Eggerth-Gagnon agar plates with horse blood (EG+HB agar plates) and expanded in liquid peptone-yeast extract-glucose (PYG) medium (Anaerobe Systems Catalog # AS-822; Morgan Hill, CA). *C. difficile* VPI 10463 (ATCC 43255) cultures were grown on Taurocholate-Cyclosporin-Cefoxitin-Fructose Agar (TCCFA) plates. All media and plates were reduced in an anaerobic environment for at least 12 h prior to use. Pure strains were struck out onto EG+HB agar plates from frozen 15% glycerol stocks and incubated inside an anaerobic chamber for 48 to 72 h. Single colonies were inoculated into 7-ml PYG media (pre-formulated, pre-reduced) and grown 24 to 48 h anaerobically at 37°C.

Experimental animals
Female 6- to 8-week-old C57BL/6 mice were purchased from Jackson Laboratories (Bar Harbor, ME) then maintained and harvested at the Mispro Biotech (Cambridge, USA) specific pathogen-free facility. All mice used in experiments were socially housed under a 12-hour light/dark cycle. Animals were 6 to 8 weeks old at the time of experiments. All animals were used in scientific experiments for the first time. All animal experiments were performed in accordance with the NIH Guide for the Care and Use of Laboratory Animals and in accordance with institutional animal care committee guidelines and regulations.

Human subjects
This phase 1a/1b, first-in-human, open-label, single-center, sequential cohort study in adult HVs was designed to evaluate the clinical safety and tolerability of VE303 at ascending doses with and without a pretreatment course of vancomycin. VE303 strain engraftment, microbiota community, and metabolite dynamics were secondary objectives. The clinical study was performed at the Pharmaron Clinical Pharmacology Center in Baltimore, Maryland. The study was approved by the IntegReview IRB in Austin, Texas and the U.S. Food and Drug Administration. The study was monitored by a safety review committee. Informed consent was obtained from all subjects. The study was registered at clinicaltrials.gov under NCT04236778.

No formal hypothesis testing was planned for this phase 1 study and accordingly, no formal sample size calculations were performed, as described in the FDA's Good Review Practices (Food and Drug Administration, 2013). The consortium of clonally derived, lyophilized, commensal bacteria in VE303 delivered in an enteric capsule was expected to have a good safety profile, given extensive prior experience with FMT. Accordingly, cohorts comprising 3 to 8 subjects were deemed adequate to address the study goals - an initial assessment of safety/tolerability and colonization dynamics after single and multiple doses of VE303. Cohorts were enrolled sequentially between December 3, 2017 and September 23, 2018; the last follow-up visit was completed on March 11, 2019. VE303 was administered at escalating single dose (Cohorts 1, 2, and 3) and multiple doses (Cohorts 4 and 5) according to pre-defined

dose-escalation guidelines at a total daily dose ranging from 1.6×10^9 to 1.1×10^{11} colony-forming units (CFU) (Table 1). Before VE303 administration, to modulate the intestinal microbiota and to determine the potential effect of residual vancomycin in the stool on VE303 colonization, oral vancomycin was administered to all subjects in Cohorts 1 through 5 (125 mg QID for 5 days), and Cohort 8 (125 mg BID for 3 days). A control cohort of subjects received only oral vancomycin. Subjects in Cohorts 1 through 5 and the vancomycin-only cohort were admitted to an inpatient unit starting on Day -1 for baseline assessment, vancomycin dosing, vancomycin washout, for the duration of VE303 dosing, and for 5 days post-dose to closely monitor the safety and tolerability of VE303 administration. Thereafter, subjects returned for outpatient follow-up visits every 2 to 4 weeks for approximately 3 months. Cohort 6 was admitted starting on Day -1 for baseline assessment and the duration of VE303 dosing. Subjects in Cohort 8 were admitted starting on Day -1 for baseline assessment and the duration of vancomycin dosing (1 to 5 days), vancomycin washout (1 day), and the first day of VE303 dosing to closely monitor the safety and tolerability of vancomycin and the first dose of VE303 administration. Subsequent doses of VE303 were administered in the outpatient clinic. After completion of VE303 dosing, subjects returned to the clinic for outpatient follow-up visits every 2 to 4 days for 1 week, and then every 2 to 4 weeks thereafter for approximately 3 months. Telephone follow-up continued for approximately 6 months following the first administration of study product for all cohorts, with additional stool collection at approximately 6 and 12 months after the first dose of VE303. Following randomization, 3 subjects from Cohorts 1, 2, and 5 were excluded due to a vancomycin-related AE, history of drug use, and non-compliance with consumption of VE303 capsules, respectively and 1 subject from Cohort 3 was lost to follow-up. Cohorts 7 and 9 were not enrolled since the study had met its objectives.

A summary of demographic and baseline subject characteristics is reported in Table 1. At screening, medical history, physical exam, vital signs, clinical laboratory measurements, and electrocardiograms (ECGs) were performed, and concomitant medications were recorded for each subject. Key inclusion criteria were male or female subjects in general good health, 18 to 60 years old, with body mass index from 18.5 to 30 kg/m^2. Key exclusion criteria were a history of clinically significant abnormality or disease, current or planned use of any products that may alter the gastrointestinal flora, gut motility, or function; prior use of fecal microbiota products; recent significant dietary changes; a history of illicit drug use; and a history of infectious disease caused by *C. difficile*, vancomycin-resistant enterococcus, multidrug-resistant organisms, hepatitis B or C, or HIV at screening. Antibiotic use before enrollment in this study was not an explicit exclusion criterion, as patients with CDI, the target population for VE303, are likely to have received one or more antibiotic courses as part of their recent treatment. Nevertheless, a review of prior and concomitant medications found that none of these HVs had received antibiotics within the 90 days before enrollment. During the study, 14 (35.9%) subjects reported use of at least one concomitant medication. Contraceptives, paracetamol, and ibuprofen were the only medications used by more than one subject. One subject in Cohort 4 received azithromycin and one subject in Cohort 1 received amoxicillin during the study.

Clinical assessment of safety was performed by a safety monitoring committee and included reporting of events by study participants, measurement of vital signs, performance of physical examinations and ECGs, and laboratory investigations. Clinical AEs were assessed using detailed, predefined scales for intensity (5-point scale) and relatedness to study treatment (6-point scale). Lab parameters included the following: complete blood count (CBC) with differential, coagulation (prothrombin time [PT]/international normalized ratio [INR] and activated partial thromboplastic in time [aPTT]), serum chemistry (sodium, potassium, chloride, carbon dioxide, albumin, alkaline phosphatase, direct and total bilirubin, alanine aminotransferase [ALT], aspartate aminotransferase [AST]), gamma-glutamyl transferase [GGT], blood urea nitrogen, calcium, creatinine, phosphorus, glucose, and lactate dehydrogenase [LDH]), C-reactive protein (CRP), erythrocyte sedimentation rate (ESR), amylase/lipase, a lipid panel (cholesterol, low-density lipoprotein [LDL], and high-density lipoprotein [HDL]), and urinalysis.

METHOD DETAILS

VE303 Genome Assembly and Taxonomic Assignment

High-quality, complete genomes were generated for each VE303 strain using Illumina plus PacBio hybrid assemblies. Genomic DNA (gDNA) was extracted from pure cultures in exponential phase of growth using the MasterPure™ Complete DNA and RNA Purification Kit (Epicentre). For Illumina sequencing, purified gDNA for each VE303 strain was fragmented using a Covaris sonicator and Illumina libraries were generated using the TruSeq DNA PCR-Free Library Prep (Illumina). The Illumina libraries were run on an Agilent bioanalyzer chip to determine the average size of the libraries. The samples were then quantitated using the Kapa Biosystems Illumina Library Quantification Real-Time PCR assay. Each library was diluted to 1 nM and pooled. The 1 nM library pool (20 μl volume) was denatured with 20 μL of 0.2 N sodium hydroxide (NaOH), diluted to a final concentration of 12 pM, and 1% of 12 pM PhiX was added prior to loading onto the MiSeq sequencer. The samples were sequenced using the Illumina V3 2 × 300 base pair (bp) protocol at the Forsyth Institute (Cambridge, MA) on the 5th of February 2016. For PacBio sequencing, libraries were prepared for sequencing on the RS II (Pacific Biosciences, Menlo Park, CA) by shearing DNA with G-tubes (Covaris), targeting an average fragment size of 20 kb. The SMRTbell Template Preparation Kit (Pacific Biosciences) was used to ligate hair-pin adapters required for sequencing to the fragmented DNA. Libraries were size-selected using the BluePippin (Sage Science, Beverly, MA) and sequenced using PacBio's P6-C4 chemistry and 240-minute movies at the University of Maryland, Institute for Genome Sciences UM-IGS (Baltimore, MD). PacBio reads were filtered using Filtlong v0.2.1 (Wick and Menzel, 2019) to remove reads shorter than 1,000 bp and keep only reads with Filtlong quality scores above the 10th percentile. Quality filtered PacBio reads were then assembled using Flye v2.9 (Kolmogorov et al., 2019), except for the

VE303-04 PacBio reads which were assembled using Raven v1.5.1 (Vaser and Šikić, 2021). Illumina reads were filtered using fastp v0.12.4 (Chen et al., 2018), and then used to polish the PacBio assemblies through two rounds of Racon v1.4.20 (Vaser et al., 2017) polishing using BWA-MEM v0.7.17 (Li, 2013) mapping results. Third and fourth rounds of short-read polishing were performed on all assemblies using Pilon v1.24 (Walker et al., 2014) and Bowtie 2 v2.2.5 (Langmead and Salzberg, 2012) mapping results. A fifth and final round of short-read polishing was performed on all assemblies using Polypolish v0.4.3 (Wick and Holt, 2022). All filtering, assembly and polishing software was run using default parameters unless otherwise specified. GTDB-Tk (Chaumeil et al., 2019) (database version 89) was used to assign the VE303 strain PacBio genomes to the nearest taxonomic relative.

Mouse *C. difficile* Susceptibility Experiments

Female 6- to 8-week-old C57BL/6 mice, purchased from The Jackson Laboratory (Bar Harbor, ME), were treated with the broad-spectrum antibiotic, cefoperazone (CPZ) (500 μg/ml), in the drinking water for 10 days followed by fresh sterile water for 2 days. Animals were split into individual treatment groups and dosed once, by oral gavage, with a 0.2-ml dose of phosphate-buffered saline (PBS) containing approximately 10^8 total bacteria, as determined by optical density (OD) at 600nm. One day later, mice were challenged with 0.2 ml of 10^4 *C. difficile* VPI 10463 (ATCC 43255) spores re-suspended in PBS by oral gavage. Weights were monitored starting on the day when *C. difficile* was inoculated and subsequently daily for the duration of the experiment. Vancomycin, a standard-of-care drug for the treatment of CDI, was included as a positive control and administered at 1 mg/mouse in 0.2 ml once daily for 7 days starting on the day of challenge. For FMT experiments, a 10% fecal slurry from human donor material preserved in PBS and 15% glycerol containing approximately 10^8 CFU of bacteria was prepared by diluting the stool in PBS. Prior to *C. difficile* challenge, 0.2 ml of this fecal suspension was administered to mice by oral gavage. VE303 efficacy was tested in 4 independent experiments, two of which included FMT as a comparison arm, whereas all other consortia were tested once (n=5 to 10 per group, per experiment). The 'No Tx' group remained untreated following cefoperazone administration or received a single dose of PBS. All animals were monitored for survival and weight change for the duration of the experiment (7 days). Mice were euthanized after losing $\geq$ 20% of baseline weight.

C. difficile in vitro Competition

All liquid mono- and co-cultures were grown in brain heart infusion broth (Becton, Dickinson and Company) under anoxic conditions. Bacterial broth cultures were grown for 24 h, then diluted to an OD_{600} of 0.1 and grown for another 2 to 3 h at 37°C to allow cultures to reach log phase. For competition with the VE303 consortium, each VE303 strain in log phase was combined in equal parts, based on OD, to reach a final consortium OD_{600} of 0.1. *C. difficile* was added to the consortium at an OD_{600} of 0.1. For competition with a single VE303 strain, the strain was diluted to a final OD_{600} of 0.1 and combined with *C. difficile* at the same OD. *Clostridium bifermentans* and *Lactobacillus ruminis* (isolated at Vedanta Biosciences from healthy human donors) were used as positive and negative controls, respectively. After the cultures were combined, they were incubated for 2 to 3 h at 37°C. Co-cultures were serially diluted 1:10, and 100 μl of dilutions were plated onto TCCFA plates. *C. difficile* colonies on the TCCFA plates were enumerated after a 48- to 72-h incubation at 37°C under anoxic conditions. Four independent experiments were completed for the competition assay of VE303 consortium against *C. difficile*, and three independent experiments were carried out for the competition assay of individual VE303 strains against *C. difficile*

In vitro SCFA Assays

Bacterial cultures were grown in 7 ml PYG broth to an OD_{600} of $\geq$ 0.2. A 100-μl sample of each culture was taken to determine bacterial concentration. Briefly, 100 μl of ten-fold serial dilutions were plated onto EG+HB agar. Plates were incubated at 48 to 72 h under anoxic conditions, then CFU enumeration was completed using the EasyCount 2 (bioMérieux SA). Filtered supernatants for SCFA analysis were obtained by centrifuging the remainder of the cultures at 1000 relative centrifugal force (RCF) for 10 min, followed by vacuum filtration using a 0.2-μm microplate filter. The filtered supernatants were aliquoted and stored at -70°C until they were shipped on dry ice to Metabolon, Inc. (Durham, NC) for bioanalysis of SCFAs (acetate, propionate, iso-butyrate, butyrate, 2-methyl-butyrate, isovalerate, valerate, and hexanoate). SCFA production by each strain was determined by dividing the SCFA concentration present in the supernatant by the $\log_{10}$CFU/ml of each strain.

Metagenomic Sequencing of rCDI Fecal Samples

Stool samples from a cohort of 73 rCDI patients treated with FMT from a pool of 10 donors were collected fresh and frozen unpreserved at -80 C. Stool samples were collected before and after FMT and a total of 144 stool samples were sequenced from the rCDI patient cohort. Microbial DNA was isolated from the frozen and thawed stool samples using an automated protocol with microbiome DNA isolation kits (PowerMag and ClearMag, MO BIO Laboratories, Inc.) on the KingFisherTM Flex instrument (Thermo Scientific). Paired-end shotgun deep sequencing (2 x 150 bp) of the prepared libraries was performed on the Illumina NextSeq System. Raw sequencing reads were quality-trimmed to an average Phred quality score of 25 using the BBTools package (Bushnell, 2014) and reads mapping to PhiX were removed. After quality filtering, the reads were de-duplicated if they were at least 98% identical over 100% of the length of the read. After quality filtering, there were an average of 40 million reads per sample. Sequencing reads which passed the quality filter were then analyzed for taxonomic classifications using the k-mer based One Codex platform (https://www.onecodex.com/).

Manufacturing Process and Drug Stability

The Current Good Manufacturing Practice (CGMP) production (Administration US Food and Drug, 2011; Dianawati et al., 2016; Jagschies et al., 2018) of VE303 started with the thawing of a Master Cell Bank (MCB) vial of an individual VE303 strain, which was inoculated into a flask and grown under anaerobic conditions in animal-free media (Reinforced Clostridial HiVeg Media, HiMedia Laboratories) as the starter culture for the production fermenter. Once the starter culture achieved its target cell density, it was transferred to the production fermenter where it was grown anaerobically in animal-free media (Reinforced Clostridial HiVeg Media), with both pH (7.00 +/- 0.20) and temperature (37.0 +/- 0.5 °C) control. Buffer exchange and bacterial concentration was performed by tangential flow filtration. Each fermented drug substance (DS) strain was then assessed for quality attributes and released if predefined specifications were met. Long-term DS storage and stability was at –80 °C.

Once all DS strains in the consortium were manufactured and released, they were blended together in a proportion based on their CFU viable counts to assure the same viable count of each bacterial strain are filled into each capsule. This active mixture was then blended with a flow agent and manually filled into enteric-coated capsules at room temperature with relative humidity $\leq$ 40% as drug product (DP). The capsules were packaged into bottles under nitrogen and heat sealed for long-term storage at -20 °C.

Both DS and DP were placed onto formal stability studies designed in compliance with ICH guidance. The VE303 DS and DP used in the phase 1 study met all predefined stability specifications; data indicating the CFU stability of the DS and combined DP at the recommended storage temperature are provided in Table S2.

Metagenomic Sequencing of VE303 Fecal Samples

Stool samples were collected fresh and approximately 250 mg was transferred to an OMNIgene-GUT tube (DNAgenotek, Ottawa, CAN) and resuspended in the preservation buffer according to manufacturer's instructions. Preserved stool suspensions were then extracted and sequenced on the Illumina NextSeq platform at DNAgenotek using standard operating procedures.

Strain Detection Algorithm for VE303

A flowchart describing the One Codex strain algorithm is included as Figure 2. Unique genomic regions for each of the VE303 organisms were identified by: 1) identifying a candidate set of overlapping k-mers (k=31bp) for each VE303 strain genome that are absent in the One Codex microbial genomes database (~40k microbes on May 4, 2016); and 2) identifying a final set of unique genomic regions (50bp windows) that were not found in any other reference genome in the One Codex database, were not found in any other VE303 strain genome, and did not share a 17bp sub-sequence with other candidate genomic regions. A total of 43,955 genomic regions satisfied these criteria, ranging from 1,539 to 10,847 per VE303 strain. This initial set of genomic regions was further refined by excluding those regions that were detected in a set of 249 healthy human stool metagenomic sequencing datasets (collected internally and from publicly available sources) and any regions that were recovered at a low rate in whole genome sequence datasets from pure cultures of the VE303 strains. Following this exclusivity testing step, a final set of 12,234 genomic markers were identified, ranging from 236 to 6,722 per VE303 strain (Table S4). Marker sequences span the entire length of VE303 strain genomes, including genes and intragenic regions. Detection of the VE303 strains from Illumina metagenomic sequencing datasets relied on these unique genomic marker regions (Figure 2). Each of the 50bp genomic regions is shorter than the sequence fragments ("reads") generated through the metagenomic sequencing process. Therefore, the unique genomic regions were detected as sub-sequences within any of the metagenomic reads. The unique genomic regions were considered detected if 1) the sequence fragment contained at least 1 perfect alignment $\geq$ 17bp to the target genomic region; and 2) the entire 50bp genomic region aligned against the sequence fragment with no more than 3 mismatches. Detection of the exact 17bp alignment was executed using a k-mer alignment approach. Sensitive alignment of the entire 50bp genome sequence was conducted using the pairwise alignment module implemented in BioPython (Cock et al., 2009). Each of the target genomic regions was considered present if there is at least one read in the input dataset that satisfies these criteria.

The presence or absence of each VE303 strain in each patient sample was determined by analyzing the number of unique genomic markers that were detected, as well as the relative abundance of each marker. Two key metrics were used to detect each VE303 strain: 1) Depth of marker recovery: the number of sequence fragments matching any marker, divided by the total number of markers; and 2) Coverage of marker recovery: the number of markers with >=1 matching sequence fragment, divided by the total number of markers. The detection of each VE303 strain was determined as follows:

"Detected" when the mean marker depth exceeded 0.1x and the coverage of markers detected exceeded a minimum threshold of two standard deviations below the mean expected from a multinomial distribution (with 25% zero inflation to account for marker dropout).

"Probable" when the mean marker depth exceeded 0.1x and the coverage of markers detected was between 2-4 standard deviations below the mean.

"Low Confidence" when the mean marker depth fell between 0.01x and 0.1x.

"Not detected" when the mean marker depth did not exceed 0.01x or the number of markers was less than four standard deviations below the expected mean.

The threshold of 0.1x was chosen as a minimum threshold for organism detection to ensure that genomic data were recovered from each organism at a level sufficient to distinguish genomic signal from near neighbors. These methods were validated for robust and

specific detection of each VE303 strain using three approaches: 1) pure VE303 gDNA spiked into human stool gDNA at decreasing percentages (Figure 2B), 2) human stool samples spiked with increasing CFUs of each VE303 strain before DNA extraction and metagenomic sequence analysis (Figure S2B), and 3) the ability to detect the VE303 strain genomes in the original host donor stool and not in unrelated control stool samples (Figure S2C). The first validation approach is described in the results (Figure 2B). In the second validation approach, each VE303 strain was cultured individually, and exponential cultures were added at increasing CFUs (ranging from 10^8 to 10^{13} CFUs per strain) to 50 to 100 mg of raw donor stool from 2 individuals. DNA was extracted and metagenomic sequencing data were generated on the Illumina platform and analyzed using the VE303 detection method. Of the 8 VE303 organisms, 7 (87.5%) were detected at all spike-in amounts. Strain VE303-03 was detected at 10^9 and 10^{10} CFUs but not at 10^8. *In silico* subsets of the *in vitro* spike in metagenomic sequences were generated ranging from as few as 25,000 reads to the full 10 to 20 million reads in the original dataset to determine the limit of strain detection. In this analysis we calculated an average LOD of 0.06% +/- 0.04% (2 SD) expressed as a normalized relative abundance for a 10 million read dataset. The VE303 strain detection assay was able to successfully detect strains VE303-05, -06, -07, and -08 in the original donor stool where they were isolated. The donor stool used to isolate VE303-01 through -04 was unavailable for analysis.

Bacterial Community Abundance and pVMRI

The estimated RA of bacterial species in the microbial community (including VE303 strains) was determined using the standard One Codex algorithm from quality-filtered metagenomic sequence reads after removal of unclassified reads and reads that map to the human host (Minot et al., 2015). At higher taxonomic levels (*e.g.,* Phylum or Class level) the RA was calculated for each sample as the ratio of sequence reads assigned at the desired taxonomic level (plus all reads assigned below) to the total number of assigned reads. We then calculated the absolute abundance of DNA for each species (or density) in the microbial community according to Equation 1

$$Abs = RA \times \frac{DNA_{\mu g}}{Stool_{mg}} \times \frac{V_B}{V_S}$$ (Equation 1)

In this Equation, *RA* equals estimated relative abundance of the bacterial taxa. $DNA_{\mu g}$ is the total DNA yield. $Stool_{mg}$ is the mass of stool collected (final mass of Omnigene gut tube – average weight of Omnigene gut tube). V_B is the volume of buffer in the Omnigene gut tube. V_S is the volume of sample in the DNA extraction . It is noteworthy to mention that this estimate is sensitive to several parameters including contributions by improper sample collection, non-bacterial DNA, stool water content, and the presence of undigested dietary components (Contijoch et al., 2019; Faith et al., 2011; Llewellyn et al., 2018; Reyes et al., 2013). All samples were collected by trained staff and by trained subjects. Comprehensive notes on tube and sample collection status were taken by staff at our CLIA-certified sequencing provider. We observed no significant spills, improper storage, or collection issues. We assessed the contribution of fungal, viral, and host DNA across all samples and it ranged between 0.056 and 1.693% of total reads per sample. Given their very small contribution, we do not believe this DNA had a significant effect on the measurement of absolute abundances of bacteria. Additionally, microbiota density may change independently of water content, implying that the density of microbes can be altered independently of water and other contents of the stool bulk, such as undigested dietary components or host tissue (Contijoch et al., 2019).

The Post-Vancomycin Microbiota Recovery Index was calculated according to Equation 2 using the Class-level RA of sequences in each metagenomic sample, as described previously (Blount et al., 2018).

$$pVMRI = \frac{\left(RA_{Bacteroidia} + RA_{Clostridia} + RA_{Actinobacteria} + RA_{Coriobacteriia}\right)}{\left(RA_{Bacilli} + RA_{\gamma Proteobacteria} + RA_{Negativicutes}\right)}$$ (Equation 2)

BA and SCFA Analysis of VE303 Fecal Samples

Stool samples were analyzed for 15 bile acids, including Cholic Acid (CA), Chenodeoxycholic Acid (CDCA), Deoxycholic Acid (DCA), Lithocholic Acid (LCA), Ursodeoxycholic Acid (UDCA), Glycocholic Acid (GCA), Glycochenodeoxycholic Acid (GCDCA), Glycodeoxycholic Acid (GDCA), Glycoursodeoxycholic Acid (GUDCA), Taurocholic Acid (TCA), Taurochenodeoxycholic Acid (TCDCA), Taurodeoxycholic Acid (TDCA), Taurolithocholic Acid (TLCA), Tauroursodeoxycholic Acid (TUDCA), and Glycolithocholic Acid (GLCA) and compared to internal standards using proprietary methods (Metabolon Inc, Durham, NC, USA). Approximately 8 to 12 mg of lyophilized human stool was used for each sample and analyzed by HPLC. The peak area of each BA is measured against the internal standards and corrected for sample weight (dry lyophilized stool). The final concentrations are provided as ng BA/mg lyophilized feces.

Stool samples were analyzed for 8 SCFAs including acetic acid, propionic acid, isobutyric acid, butyric acid, 2-methyl-butyric acid, isovaleric acid, valeric acid, and caproic acid (hexanoic acid) and compared to internal standards using proprietary methods (Metabolon Inc, Durham, NC, USA). Approximately 100 mg of human stool was used for each sample and analyzed by LC-MS/MS. The peak area of each SCFA is measured against the internal standards and corrected for sample weight (wet stool). The final concentrations are provided as ng SCFA/mg feces.

Bile Acid Gene Prediction in VE303 Genomes

We built a custom database of secondary BA metabolism enzymes by first downloading from Uniprot all the sequences corresponding to each step involved in BAs transformation according to Heinken et al. (2019), and running CD-Hit (Fu et al., 2012) to remove redundant sequences at 90% identity using parameters as stated by Heinken et al. (2019). To determine potential contribution to secondary BA metabolism, the assembled genome for each of the 8 VE303 strains was annotated with PROKKA (Seemann, 2014). The resulting predicted protein coding sequences for each strain were then mapped against the custom BA metabolism database using reciprocal best-hit analysis (https://github.com/peterjc/galaxy_blast) which is part of the NCBI BLAST+ Galaxy integrated toolset (Cock et al., 2015). The organisms *Clostridium hylemonae*, *Clostridium hiranonis*, *Clostridium scindens* and *Eggerthella lenta* have been documented to have a role in secondary BA production (Devlin and Fischbach, 2015; Doden et al., 2018; Heinken et al., 2019; Kang et al., 2019; Ridlon et al., 2010, 2016) – we included these genomes as positive controls to validate our BA gene prediction approach and interpret predicted functions within VE303 genomes.

QUANTIFICATION AND STATISTICAL ANALYSIS

Animal Model Statistical Analysis

Statistical significance was assessed by the two-tailed Student's t-test for *C. difficile* suppression *in vitro*, Holm-Sidak test for weight measurements and the log-rank test for survival. Statistical analyses were performed using Prism GraphPad software v8.0 (https://www.graphpad.com/scientific-software/prism/).

Analysis of VE303 Related Species in rCDI Patients

A relative abundance threshold of 0.01% was utilized to filter out noisy taxonomic assignments. For each FMT recipient, a single representative sample was chosen pre- and post-FMT based on closest proximity of the sample's collection date to the FMT administration date to conduct the analysis. Recipients were excluded from the analysis if a sequenced sample from either pre- or post-FMT timepoints was unavailable. Zero-Inflated Beta Random Effect (ZIBR) model; https://github.com/chvlyl/ZIBR (Chen and Li, 2016) was used to simultaneously model abundance (beta regression) and prevalence (logistic regression) of microbial taxa in recipients, while including a random effect to account for repeated measurements on the same subject.

$$Taxa \sim treatment + Donor + Response + 1|Subject$$

The dataset was tested for significant associations between recipient microbial taxa and treatment, response to FMT, and Donor group. Significance was set at $\alpha=0.05$, adjusted for multiple hypotheses with false discovery rate (FDR) correction.

VE303 Colonization in Clinical Samples

Stool samples were used to assess VE303 detection on study collection days 0, 5, 6, 7 and 8, and at weeks 4, 6, 8, 12, and 52. When VE303 dosing was postponed to accommodate vancomycin administration (Cohorts 1 to 5), the times used in the analysis were defined relative to the start of VE303 administration. VE303 detection was defined as the sum of the relative abundance of each bacterial strain at each discrete sample collection. A noncompartmental method was used to generate detection metrics for the absolute concentrations of the VE303 consortium. The AUC was calculated first by fitting a logistic curve to the strain concentrations up to day 60 using code adapted from the growthcurver package in R (Sprouffske and Wagner, 2016). The acute colonization over the first 20 days of treatment was computed as the area under the logistic curve by integrating the curve from day 0 to day 20. Statistical differences in AUC between cohorts and strains were performed using Kruskal-Wallis test followed by the Dunn pairwise post-hoc test with the Holm correction ('FSA' package version 0.9.1).

Determination of *Clostridia* displaced by VE303

To assess displacement of native Clostridia by VE303 in recipients, we identified species that showed sustained suppression in abundance compared with their baseline abundance and were negatively associated with VE303. We ran a mixed effects regression model to identify all Firmicutes that were depleted in abundance post-dosing (Day 14 to Day 30) compared with baseline. The arcsin-transformed RA of each species was modeled as a function of time (Baseline/Post VE303), including the cohort nested with subject ID as a random effect: $abundance \sim Time\left(\frac{Baseline}{Post-VE303}\right) + \left(\frac{pID}{CohortID}\right)$. Next, we identified all species that were negatively associated with VE303 (Day 14 to Day 50): $abundance \sim Time + Total\ VE303 + \left(\frac{pID}{CohortID}\right)$. Clostridia that were significant in both models were considered to have been displaced by VE303 (Figure S4E).

Microbiota and Metabolite LME Modeling

To identify BAs that were affected by VE303 administration, we conducted linear mixed effect modeling of the form $analyte \sim Treatment + VE303 + \left(\frac{pID}{CohortID}\right)$. Here, *analyte* corresponds to the BA measured density in an individual at a time point (day), *Treatment* is a categorical variable to describe if the measurement was taken before, during or after vancomycin treatment, *VE*303 corresponds to the total RA of VE303 in a sample after vancomycin administration, *pID* and *CohortID* label individual subjects and study cohort, respectively. For *Treatment* we used baseline samples as the pre-vancomycin samples. Since data are repeated samples from different subjects that are subdivided into cohorts, we used $\frac{pID}{CohortID}$ as a nested random effect. Metabolites with a

p-value associated with *Treatment* : *during* − *vancomycin* smaller than 0.05 are considered significantly affected by vancomycin treatment. Metabolites with p-value associated to *Treatment* : *post* − *vancomycin* smaller than 0.05 are considered significantly affected by vancomycin post-treatment and in the absence of VE303 (e.g., only vancomycin cohort). Metabolites with p-value associated to *ve*303 smaller than 0.05 are significantly affected by total VE303 abundance post treatment.

Microbiota and Metabolite Random Forest Regression

We conducted Random Forest Regression (RFR) to determine the effect of the VE303 strains on BA and SCFA dynamics post-vancomycin and to predict metabolite abundance as a function of the resident bacteria and VE303 strain abundances. To address the issue of repeated sampling, we followed an approach as previously described (Haran et al., 2019). Briefly, we generated 100 randomly selected sample subsets, where each subset includes at least one sample per individual. The random forest model was run on 30 different random seeds on each subset of the data. We ranked microbes (both resident bacteria and VE303 strains) based on their permutated variable importance value (Altmann et al., 2010) across the 30x100 RFR realizations. Variable importance does not indicate whether a feature positively or negatively affects the predicted variable; we generated Accumulated Local Effects (ALE) Plots (Apley and Zhu, 2020) to determine the relationship between metabolites and microbial abundance. Computed using conditional probability distributions, ALE plots provide an unbiased way to determine the individual effects of a set of strongly correlated features on the response variable. We used the slope of the log-log transformed ALE plots as a measure for average feature effect. Inferred coefficients summarized an overall positive or negative effect on metabolite abundance and shown as a clustered heatmap.

ADDITIONAL RESOURCES

Details on the Phase 1a/1b trial are available at clinicaltrials.gov under NCT04236778 (https://clinicaltrials.gov/ct2/show/NCT04 236778).